

Article

The Lignicolous Genus *Entonaema*: Its Phylogenetic–Taxonomic Position within *Hypoxylaceae* (*Xylariales*, *Fungi*) and an Overview of Its Species, Biogeography, and Ecology

Ana Pošta, Neven Matočec , Ivana Kušan * , Zdenko Tkalčec and Armin Mešić 

Laboratory for Biological Diversity, Ruđer Bošković Institute, Bijenička Cesta 54, HR-10000 Zagreb, Croatia; aposta@irb.hr (A.P.); nmatocec@irb.hr (N.M.); ztkalcec@irb.hr (Z.T.); amesic@irb.hr (A.M.)

* Correspondence: ikusan@irb.hr

Abstract: The lignicolous saprotrophic genus *Entonaema* contains six formally accepted species: *E. liquescens* (type species), *E. cinnabarinum*, *E. globosum*, *E. dengii*, *E. moluccanum*, and *E. siamensis*. Its stromatic ascomata develop on the surface of dead wood remnants; they are rather large, globose to irregularly shaped, and vividly coloured. The fresh stroma interior is filled with a liquid matter. In early studies, the genus was considered to have a preference for tropical habitats, while in more recent field research, numerous collections have been added from warm, temperate areas of Europe, North America, and Asia. Our taxonomic and phylogenetic studies were based on freshly collected *E. cinnabarinum* from Croatia and *E. liquescens* from the USA. A phylogenetic study of the sequence alignment of four concatenated gene regions (ITS, LSU, *rpb2*, and β -*tub*) revealed the true taxonomic position of *Entonaema* within *Hypoxylaceae* (*Xylariales*), a sister to *Hypoxylon carneum*. Detailed macroscopic and microscopic descriptions of *E. cinnabarinum* are accompanied by drawings and colour photographs, while the study of *E. liquescens* is focused on stomatal microchemical reaction. With new information, the worldwide identification key to the putative species of *Entonaema* is proposed. Ecological data and biogeographical patterns were studied using all available and reliable sources of recorded data. Climatic preferences of the two most widespread *Entonaema* species, *E. liquescens* and *E. cinnabarinum*, are discussed in detail.

Keywords: biodiversity; climatic shift; key to the species; phylogeny; *Sordariomycetes*; taxonomy



Citation: Pošta, A.; Matočec, N.; Kušan, I.; Tkalčec, Z.; Mešić, A. The Lignicolous Genus *Entonaema*: Its Phylogenetic–Taxonomic Position within *Hypoxylaceae* (*Xylariales*, *Fungi*) and an Overview of Its Species, Biogeography, and Ecology. *Forests* **2023**, *14*, 1764. <https://doi.org/10.3390/f14091764>

Academic Editors: Carolina Girometta and Giancarlo Angeles Flores

Received: 16 July 2023

Revised: 15 August 2023

Accepted: 22 August 2023

Published: 31 August 2023



Copyright: © 2023 by the authors. Licensee MDPI, Basel, Switzerland. This article is an open access article distributed under the terms and conditions of the Creative Commons Attribution (CC BY) license (<https://creativecommons.org/licenses/by/4.0/>).

1. Introduction

The genus *Entonaema* Möller was established in 1901 [1], represented by *E. liquescens* Möller as a type species and *E. mesentericum* Möller as an additional species of the genus. The latter species was later justifiably removed from the genus [2]. The genus was retained as a member of *Xylariaceae* Tul. & C. Tul. in the same study, a taxonomic view supported by the majority of taxonomists (e.g., [3–9]). Recently, after detailed molecular phylogenetic study with a sufficient amount of xylarialean DNA sequences, *Entonaema* was assigned to the newly resurrected and emended family *Hypoxylaceae* DC [10].

As with the majority of xylarialean fungi, the genus is characterised by its lignicolous way of life [8], developing rather large, globose to irregularly shaped, vividly coloured stromata on the surface of dead wood remnants; the intact interior of the stroma is filled with a liquid matter, while the perithecial layer is subgelatinous when fresh but coriaceous and hard when dried. The perithecia are inserted into the stomatal cortex; they are monostichous and carbonaceous, and they contain cylindrical, pedicellate asci with an amyloid apical ring. Ascospores are one-celled, brownish, and equipped with a longitudinal germ slit exceeding one-half of the spore's length. Besides *E. liquescens*, five more species are accepted in the genus today: *E. cinnabarinum* (Cooke & Masee) Lloyd [11], *E. dengii* J.D. Rogers [5], *E. moluccanum* J.D. Rogers [5], *E. globosum* R. Heim [12], and *E. siamensis* Sihan., Thienh. & Whalley [13]. Only two out of the six species currently belonging to the genus

are biogeographically widespread, viz., *E. liquescens* and *E. cinnabarinum*. To date, a true phylogenetic position of the genus was, however, a matter of uncertainty [10,14,15]. Our study was significantly concentrated on the phylogenetic analyses as well as the stromatal pigments and anatomy of the newly collected, living material of the two aforementioned typical and most widespread *Entonaema* species in order to reveal the true affinities of the genus. The analysis of their ecological–biogeographical traits was conducted on the basis of all accessible and verifiable records worldwide, and their climatic preferences are discussed in detail. The worldwide identification key to the putative species of *Entonaema* is proposed.

2. Materials and Methods

2.1. Microscopic Studies

Microscopic characteristics based on living cells and tissues (*) were recorded using vital taxonomy methods [16], while those based on dead cells and tissues (+) were obtained from fixed fresh and dry materials. All described microscopic elements were observed in tap water (H₂O), and cytochemical and histochemical data were additionally observed in Lugol's solution (IKI), Brilliant Cresyl Blue (CRB), potassium hydroxide (5% and 10% KOH), and Cotton Blue (CB). Microscopic elements were studied with a Zeiss Axioskop 40 FL (Carl Zeiss AG, Oberkochen, Germany) transmission light microscope (bright-field, phase-contrast, and dark-field techniques) under magnifications up to 1000×. Drawings were made freehand to scale, and microphotographs were taken with Nikon D750 and Nikon Z6 (Nikon Corporation, Tokyo, Japan) cameras mounted on the camera adapter T2-T2 SLR 2.5× (Carl Zeiss AG, Oberkochen, Germany) attached to the microscope's trinocular tube. Characters of stromatal and hymenial elements were based on a minimum of three stromata from each collection. Spore measurements were based on samples of 150 fully mature, normally developed, living, and randomly selected ascospores. Measurements were taken directly using an ocular micrometre and from microphotographs using PIXIMÈTRE software ver. 5.10 [17] to an accuracy of 0.1 µm. Length, width, and length/width ratio ("Q" value) were given as follows: (min.) stat. min.—stat. mode—stat. max. (max.), where "min." = minimum (lowest measured value), "stat. min." = statistical minimum (arithmetic mean minus two times standard deviation), "stat. mode" = statistical mode, "stat. max." = statistical maximum (arithmetic mean plus two times standard deviation), and "max." = maximum (highest measured value). The dried material was deposited at the Croatian National Fungarium (CNF), Zagreb, Croatia.

2.2. Axenic Cultures

Ascospore germination of *E. cinnabarinum* was tested by inoculation of freshly ejected ascospores on potato dextrose agar (PDA, HiMedia Laboratories Pvt. Ltd., Mumbai, India), malt extract agar (MEA, HiMedia Laboratories Pvt. Ltd., Mumbai, India), and oatmeal agar (OA, after Samson et al. [18]), both with and without pretreatment with hydrochloric acid (pH = 3.3; 0.0005 M HCl) for two hours at 25 °C. Petri dishes were kept at 24 °C in the dark for 7 days.

2.3. DNA Extraction, PCR Amplification, and Sequencing

Genomic DNA was extracted from fresh tissue of stromata using an EZNA[®] HP Fungal DNA Kit (Omega Bio-tek, Norcross, GA, USA) following the manufacturer's protocol, with time adjustment of lysis incubation to 1 h. Four gene regions, ITS (internal transcribed spacer region), LSU (28S large subunit of ribosomal DNA), *rpb2* (second largest subunit of the DNA-directed RNA polymerase II), and *β-tub* (beta-tubulin), were amplified using primer pairs ITS1F/ITS4 [19,20], LR0R/LR7 [21], RPB2-5F/RPB2-7cR [22], and T1/T2, T11/T22 [23], respectively. The 25 µL PCR mixtures contained 9.5 µL of ddH₂O, 12.5 µL of GoTaq[®] G2 Green Master Mix (Promega, Madison, WI, USA), 1 µL of DNA template, and 1 µL of each forward and reverse primer with a final concentration of 0.2 µM, respectively. The PCR amplification for ITS and LSU gene regions was performed using a touchdown

program: initial denaturation at 95 °C for 2 min; followed by 5 cycles of denaturation at 95 °C for 30 s, annealing at 55 °C for 45 s (add -1 °C per cycle), extension at 72 °C for 1.5 min; 30 cycles of denaturation at 95 °C for 30 s, annealing at 52 °C for 45 s, extension at 72 °C for 1.5 min; and a final extension at 72 °C for 5 min. The PCR amplification of *rpb2* was set up as described by Liu et al. [22], and of *β -tub* as described by O'Donnell and Cigelnik [23]. Successful PCR products were purified using ExoSAP-IT™ (Thermo Fisher Scientific, Waltham, MA, USA) cleanup reagent following the manufacturer's protocol and sent to Macrogen Europe (Amsterdam, The Netherlands) for bidirectional Sanger sequencing.

2.4. Sequence Alignment and Phylogenetic Analysis

Sequence reads were assembled and edited using Geneious Prime 2023.0.4. (<https://www.geneious.com>, Biomatters, Auckland, New Zealand, accessed on 18 October 2022). Assembled sequences were deposited at the National Center for Biotechnology Information (NCBI) GenBank database.

A phylogenetic dataset comprised of 501 sequences of four gene regions (ITS, LSU, *rpb2*, *β -tub*) from 142 taxa was selected for further analyses (Table 1). The listed species of *Hypoxylaceae*, *Xylariaceae* and *Graphostromataceae* M.E. Barr, J.D. Rogers & Y.M. Ju in Table 1 originated from previously published studies. All published sequences from NCBI Nucleotide database resulting with '*Entonema*' as the genus name were also included in phylogenetic analyses. Sequences were aligned by each gene region using MAFFT v7.450 [24,25] available as a Geneious Prime plugin. After being aligned and trimmed, concatenation of ITS, LSU, *rpb2* and *β -tub* alignments was accomplished using Geneious Prime 2023.0.4. Concatenated alignment contained 5794 characters positions including gaps, with 974 character positions for ITS, 1778 characters positions for LSU, 1065 characters positions for *rpb2*, and 1977 characters positions for *β -tub*. *Pyriformiascoma trilobatum* Daranag., Camporesi & K.D. Hyde, *Diatrype disciformis* (Hoffm.) Fr., *Creosphaeria sassafras* Y.M. Ju, F. San Martín & J.D. Rogers, and *Calceomyces lacunosus* Udagawa & S. Ueda were selected as the outgroup for phylogenetic analyses following Wendt et al. [10].

Phylogenetic analyses were conducted using Maximum Likelihood (ML) analysis in IQ-TREE v1.6.12 [26,27] and a Bayesian Inference (BI) analysis in MrBayes 3.2.6 (Geneious plugin, [28]). The best model was selected by ModelFinder implemented in IQ-TREE separately considering the corrected Akaike, and Bayesian Information Criterion (cAIC, BIC). TIM2+F+I+G4 was selected as best model for both phylogenetic datasets. ML analysis was executed by applying the ultrafast bootstrap approximation with 1000 replicates. BI analysis was executed for 5,000,000 generations, sampling trees and other parameters every 1000 generations. The default numbers of chains (four) and heating parameters were used. Posterior probabilities (BPP) were calculated after burning the first 25% of the posterior sample. Phylogenetic trees were visualized and annotated using iTOL v6.5.4 [29] and FigTree 1.4.3 (<http://tree.bio.ed.ac.uk/software/figtree/>, accessed on 22 October 2023).

2.5. The Analysis of Ecological and Biogeographical Traits

A thorough inspection of currently accessible information on *Entonaema* species record data revealed a huge potential because each of the previous studies has always treated only a very limited amount of collections. Record data were taken from all available scientific publications known to the authors and from the online database GBIF (www.gbif.org, accessed on 26 June 2023), as well as the data derived from our own research and that of our colleagues, as a source for better understanding of the species ecology and biogeography. Only those records that were identified by specialists or were accompanied with high quality macrophotographs showing certain *Entonaema* species and stromatal ontogeny were accepted for the analysis. Additionally, the record should have had a precise locality name or assigned geographic coordinates, accompanied with a record date to ascertain species phenology. This was a prerequisite for obtaining ecological data (habitat type,

vicinity of water bodies, elevation, etc.) for each record, using Google Earth Pro 7.3.6.9345 (Google LLC, Mountain View, CA, USA) software.

The same software was used to visualize ‘Global_1986-2010_KG_5m.kmz’ digital layer downloaded from <https://koeppen-geiger.vu-wien.ac.at/present.htm> (accessed on 26 June 2023) in order to ascribe the current Köppen–Geiger climate type to every *Entonaema* record for climatic characterisation. Obtained data were also compared to an older worldwide Köppen–Geiger climate classification made by Kottek et al. [30]. Abbreviations of climatic types follow the same reference.

Table 1. Species included in this study, associated voucher numbers, countries of origin, and GenBank accession numbers. Newly generated sequences are marked in bold. Abbreviations: HT = holotype, ET = epitype, IT = isotype, PT = paratype.

Taxa	Voucher	Country	ITS	LSU	<i>rpb2</i>	<i>β-tub</i>	Ref
<i>Amphirosellinia fushanensis</i>	HAST 91111209 HT	Taiwan	GU339496	N/A	GQ848339	GQ495950	[31]
<i>Annulohypoxyylon annulatum</i>	CBS 140775 ET	Texas	KY610418	KY610418	KY624263	KX376353	[10,32]
<i>Annulohypoxyylon atroroseum</i>	ATCC 76081	Thailand	AJ390397	KY610422	KY624233	DQ840083	[10,33]
<i>Annulohypoxyylon michelianum</i>	CBS 119993	Spain	KX376320	KY610423	KY624234	KX271239	[10,32]
<i>Annulohypoxyylon moriforme</i>	CBS 123579	France	KX376321	KY610425	KY624289	KX271261	[10,32]
<i>Annulohypoxyylon nitens</i>	MFLUCC 12-0823	Thailand	KJ934991	KJ934992	KJ934994	KJ934993	[34]
<i>Annulohypoxyylon stygium</i>	MUCL 54601	France	KY610409	KY610475	KY624292	KX271263	[10]
<i>Annulohypoxyylon truncatum</i>	CBS 140778 ET	Texas	KY610419	KY610419	KY624277	KX376352	[10,32]
<i>Astrocystis concavispora</i>	MFLUCC 14-0174	Italy	KP297404	KP340545	KP340532	KP406615	[34]
<i>Biscogniauxia arima</i>	WSP 122 IT	Mexico	EF026150	N/A	GQ304736	AY951672	[31]
<i>Biscogniauxia nummularia</i>	MUCL 51395 ET	France	KY610382	KY610427	KY624236	KX271241	[10]
<i>Brunneiperidium gracilentum</i>	MFLUCC 14-0011 HT	Italy	KP297400	KP340542	KP340528	KP406611	[34]
<i>Calceomyces lacunosus</i>	CBS 633.88 HT	Japan	KY610397	KY610476	KY624293	KX271265	[10]
<i>Camillea obularia</i>	ATCC 28093	Puerto Rico	KY610384	KY610429	KY624238	KX271243	[10]
<i>Collodiscula fangjingshanensis</i>	GZU H0109 HT	China	KR002590	KR002591	KR002592	KR002589	[35]
<i>Creosphaeria sassafras</i>	STMA 14087	Argentina	KY610411	KY610468	KY624265	KX271258	[10]
<i>Daldinia andina</i>	CBS 114736 HT	Ecuador	AM749918	KY610430	KY624239	KC977259	[10,33,36]
<i>Daldinia bambusicola</i>	CBS 122872 HT	Thailand	KY610385	KY610431	KY624241	AY951688	[10,37]
<i>Daldinia caldariorum</i>	MUCL 49211	France	AM749934	KY610433	KY624242	KC977282	[10,33,36]
<i>Daldinia concentrica</i>	CBS 113277	Germany	AY616683	KY610434	KY624243	KC977274	[10,14,33]
<i>Daldinia dennisii</i>	CBS 114741 HT	Australia	JX658477	KY610435	KY624244	KC977262	[10,33,38]
<i>Daldinia eschscholtzii</i>	MUCL 45435	Benin	JX658484	KY610437	KY624246	KC977266	[10,33,38]
<i>Daldinia loculatooides</i>	CBS 113279 ET	UK	AF176982	KY610438	KY624247	KX271246	[10,39]
<i>Daldinia macaronesica</i>	CBS 113040 PT	Spain	KY610398	KY610477	KY624294	KX271266	[10]
<i>Daldinia petriniae</i>	MUCL 49214 ET	Austria	AM749937	KY610439	KY624248	KC977261	[10,33,36]
<i>Daldinia placentiformis</i>	MUCL 47603	Mexico	AM749921	KY610440	KY624249	KC977278	[10,33,36]
<i>Daldinia pyrenaica</i>	MUCL 53969	France	KY610413	KY610413	KY624274	KY624312	[10]
<i>Daldinia steglichii</i>	MUCL 43512 PT	Papua New Guinea	KY610399	KY610479	KY624250	KX271269	[10]
<i>Daldinia theissenii</i>	CBS 113044 PT	Argentina	KY610388	KY610441	KY624251	KX271247	[10]
<i>Daldinia vernicosa</i>	CBS 119316 ET	Germany	KY610395	KY610442	KY624252	KC977260	[10,33]

Table 1. Cont.

Taxa	Voucher	Country	ITS	LSU	rpb2	β -tub	Ref
<i>Diatrype disciformis</i>	CBS 197.49	Netherlands	N/A	DQ470964	DQ470915	N/A	[40]
<i>Entonaema cinnabarinum</i>	agtS377	Germany	AY616685	N/A	N/A	N/A	[14]
<i>Entonaema cinnabarinum</i>	CNF 2/11046	Croatia	OQ863621	OQ863622	OQ877102	OQ877113	This study
<i>Entonaema cinnabarinum</i>	CNF 2/11047	Croatia	OQ863735	OQ864983	OQ877103	OQ877114	This study
<i>Entonaema cinnabarinum</i>	CNF 2/11052	Croatia	OQ864984	OQ865000	OQ877104	OQ877115	This study
<i>Entonaema cinnabarinum</i>	CNF 2/11053	Croatia	OQ869782	OQ869785	OQ877105	OQ877116	This study
<i>Entonaema liquescens</i>	ATCC 46302	USA	KY610389	KY610443	KY624253	KX271248	[10]
<i>Entonaema liquescens</i>	agtS279	Germany	AY616686	N/A	N/A	N/A	[14]
<i>Entonaema liquescens</i>	CNF 2/11263	USA	OQ869784	OQ865124	OQ877106	OQ877117	This study
<i>Entonaema liquescens</i>	S.D. Russell iNaturalist # 91210856	USA	OM972573	N/A	N/A	N/A	[41]
<i>Entonaema pallida</i>	PP92a	Peru	FJ884093	FJ890379	N/A	N/A	[42]
<i>Entonaemasp.</i>	JHGB08 1A	Peru	MH267933	N/A	N/A	N/A	[43]
<i>Entonaemasp.</i>	AHB18 5B	Peru	MH267934	N/A	N/A	N/A	[43]
<i>Entonaemasp.</i>	F5071	Panama	KF746156	N/A	N/A	N/A	[44]
<i>Entonaema splendens</i>	KA12-1283	South Korea	KR673521	N/A	N/A	N/A	[45]
<i>Euepixylon sphaerostomum</i>	JDR 261	USA	GU292821	N/A	GQ844774	GQ470224	[31]
<i>Graphostroma platystomum</i>	CBS 270.87 HT	France	JX658535	DQ836906	KY624296	HG934108	[10,38,46,47]
<i>Hypocreodendron sanguineum</i>	JDR 169	Mexico	GU322433	N/A	GQ844819	GQ487710	[31]
<i>Hypoxyylon addis</i>	MUCL 52797 HT	Ethiopia	KC968931	N/A	N/A	KC977287	[33]
<i>Hypoxyylonaff. rubiginosum</i>	MUCL 57724	Iran	MT214999	MT214994	MT212237	MT212241	[48]
<i>Hypoxyylonaff. rubiginosum</i>	MUCL 57725	Iran	MT215000	MT214995	MT212238	MT212242	[48]
<i>Hypoxyylon baihualingense</i>	FCATAS 477 HT	China	MG490190	N/A	N/A	MH790276	[49]
<i>Hypoxyylon bellicolor</i>	UCH 9543	Panama	MN056425	N/A	N/A	MK908139	[50]
<i>Hypoxyylon carneum</i>	MUCL 54177	France	KY610400	KY610480	KY624297	KX271270	[10]
<i>Hypoxyylon cercidicola</i>	CBS 119009	France	KC968908	KY610444	KY624254	KC977263	[10,33]
<i>Hypoxyylon chrysalidosporum</i>	FCATAS 2710 HT	China	OL467294	OL615106	OL584222	OL584229	[51]
<i>Hypoxyylon crocopleum</i>	CBS 119004	France	KC968907	KY610445	KY624255	KC977268	[10,33]
<i>Hypoxyylon crocopleum</i>	CNF 2/11316	Croatia	OQ865120	OQ869786	OQ877107	OQ877118	This study
<i>Hypoxyylon crocopleum</i>	CNF 2/11317	Croatia	OQ865187	OQ869787	OQ877108	OQ877119	This study
<i>Hypoxyylon cyclobalanopsidis</i>	FCATAS 2714 HT	China	OL467298	OL615108	OL584225	OL584232	[51]
<i>Hypoxyylon damuense</i>	FCATAS 4207 HT	China	ON075427	ON075433	ON093251	ON093245	[52]
<i>Hypoxyylon damuense</i>	FCATAS 4321	China	ON075428	ON075434	ON093252	ON093246	[52]
<i>Hypoxyylon duranii</i>	YMJ 85	China	JN979414	N/A	N/A	AY951714	[37]
<i>Hypoxyylon eurasiaticum</i>	MUCL 57720 HT	Iran	MW367851	N/A	MW373852	MW373861	[53]
<i>Hypoxyylon fendleri</i>	MUCL 54792	France	KF234421	KY610481	KY624298	KF300547	[10,33]
<i>Hypoxyylon fragiforme</i>	MUCL 51264 ET	Germany	KC477229	KM186295	KM186296	KX271282	[10,34,54]
<i>Hypoxyylon fraxinophilum</i>	MUCL 54176 ET	France	KC968938	N/A	N/A	KC977301	[33]
<i>Hypoxyylon fuscum</i>	CBS 113049 ET	France	KY610401	KY610482	KY624299	KX271271	[10]

Table 1. Cont.

Taxa	Voucher	Country	ITS	LSU	rpb2	β -tub	Ref
<i>Hypoxyylon griseobrunneum</i>	CBS 331.73 HT	India	KY610402	KY610483	KY624300	KC977303	[10,33]
<i>Hypoxyylon guilanense</i>	MUCL 57726 HT	Iran	MT214997	MT214992	MT212235	MT212239	[48]
<i>Hypoxyylon haematostroma</i>	MUCL 53301 ET	France	KC968911	KY610484	KY624301	KC977291	[10,33]
<i>Hypoxyylon howeanum</i>	MUCL 47599	Germany	AM749928	KY610448	KY624258	KC977277	[10,33,36]
<i>Hypoxyylon howeanum</i>	CNF 2/11315	Croatia	OQ865216	OQ865215	OQ877109	OQ877120	This study
<i>Hypoxyylon hypomiltum</i>	MUCL 51845	France	KY610403	KY610449	KY624302	KX271249	[10]
<i>Hypoxyylon investiens</i>	CBS 118183	Malaysia	KC968925	KY610450	KY624259	KC977270	[10,33]
<i>Hypoxyylon isabellinum</i>	STMA10247 HT	France	KC968935	N/A	N/A	KC977295	[33]
<i>Hypoxyylon lateripigmentum</i>	MUCL 53304 HT	France	KC968933	KY610486	KY624304	KC977290	[10,33]
<i>Hypoxyylon lenormandii</i>	CBS 119003	Ecuador	KC968943	KY610452	KY624261	KC977273	[10,33]
<i>Hypoxyylon liviae</i>	CBS 115282 ET	Norway	NR155154	N/A	N/A	KC977265	[33]
<i>Hypoxyylon macrosporium</i>	YMJ 47	Canada	N/A	N/A	N/A	AY951736	[37]
<i>Hypoxyylon monticulosum</i>	MUCL 54604 ET	France	KY610404	KY610487	KY624305	KX271273	[10]
<i>Hypoxyylon musceum</i>	MUCL 53765	France	KC968926	KY610488	KY624306	KC977280	[10,33]
<i>Hypoxyylon notatum</i>	YMJ 250	USA	JQ009305	N/A	N/A	AY951739	[37]
<i>Hypoxyylon ochraceum</i>	MUCL 54625 ET	France	KC968937	N/A	KY624271	KC977300	[10,33]
<i>Hypoxyylon papillatum</i>	ATCC 58729 HT	USA	KC968919	KY610454	KY624223	KC977258	[10,33]
<i>Hypoxyylon perforatum</i>	CBS 115281	France	KY610391	KY610455	KY624224	KX271250	[10]
<i>Hypoxyylon petriniae</i>	CBS 114746 HT	France	NR155185	KY610491	KY624279	KX271274	[10,32]
<i>Hypoxyylon pilgerianum</i>	STMA 13455	France	KY610412	KY610412	KY624308	KY624315	[10]
<i>Hypoxyylon porphyreum</i>	CBS 119022	France	KC968921	KY610456	KY624225	KC977264	[10,33]
<i>Hypoxyylon pseudodefndleri</i>	MFLUCC 11-0639 HT	Thailand	KU940156	KU863144	N/A	N/A	[55]
<i>Hypoxyylon pseudofuscum</i>	KR:0005879 HT	Germany	MW367857	MW367848	MW373858	MW373867	[53]
<i>Hypoxyylon pulicidum</i>	CBS 122622 HT	France	JX183075	KY610492	KY624280	JX183072	[10,56]
<i>Hypoxyylon rickii</i>	MUCL 53309 ET	France	KC968932	KY610416	KY624281	KC977288	[10,33]
<i>Hypoxyylon rubiginosum</i>	MUCL 52887 ET	Germany	KC477232	KY610469	KY624266	KY624311	[10,54]
<i>Hypoxyylon rubiginosum</i>	MUCL 57727	Iran	MT214998	MT214993	MT212236	MT212240	[48]
<i>Hypoxyylon samuelsii</i>	MUCL 51843 ET	France	KC968916	KY610466	KY624269	KC977286	[10,33]
<i>Hypoxyylon shearii</i> var. <i>minor</i>	YMJ 29	Mexico	EF026142	N/A	N/A	AY951753	[31,37]
<i>Hypoxyylon sporistriataticum</i>	UCH 9542 HT	Panama	MN056426	N/A	N/A	MK908140	[50]
<i>Hypoxyylon submonticulosum</i>	CBS 115280	France	KC968923	KY610457	KY624226	KC977267	[10,33]
<i>Hypoxyylon texense</i>	DSM 107933 HT	USA	MK287536	MK287548	MK287561	MK287574	[57]
<i>Hypoxyylon ticinense</i>	CBS 115271	France	JQ009317	KY610471	KY624272	AY951757	[10,37]
<i>Hypoxyylon ticinense</i>	CNF 2/11314	Croatia	OQ869783	OQ865219	OQ877110	OQ877121	This study
<i>Hypoxyylon trugodes</i>	MUCL 54794 ET	Sri Lanka	KF234422	KY610493	KY624282	KF300548	[10,33]
<i>Hypoxyylon ulmophilum</i>	YMJ 350	Russia	JQ009320	N/A	N/A	AY951760	[37]
<i>Hypoxyylon vogesiacum</i>	CBS 115273	France	KC968920	KY610417	KY624283	KX271275	[10,32,33]
<i>Hypoxyylon wujiangense</i>	GMBC0213 HT	China	MT568854	MT568853	MT585802	MT572481	[58]
<i>Hypoxyylon wuzhishanense</i>	FCATAS 2708 HT	China	OL467292	OL615104	OL584220	OL584227	[51]
<i>Hypoxyylon wuzhishanense</i>	FCATAS 2709	China	OL467293	OL615105	OL584221	OL584228	[51]
<i>Hypoxyylon zangii</i>	FCATAS 4029 HT	China	ON075423	ON075429	ON093247	ON093241	[52]

Table 1. Cont.

Taxa	Voucher	Country	ITS	LSU	<i>rpb2</i>	<i>β-tub</i>	Ref
<i>Hypoxylon zangii</i>	FCATAS 4319	China	ON075424	ON075430	ON093248	ON093242	[52]
<i>Jackrogersella cohaerens</i>	CBS 119126	Germany	KY610396	KY610497	KY624270	KY624314	[10]
<i>Jackrogersella minutella</i>	CBS 119015	Portugal	KY610381	KY610424	KY624235	KX271240	[10,32]
<i>Jackrogersella multiformis</i>	CBS 119016 ET	Germany	KC477234	KY610473	KY624290	KX271262	[10,32,33]
<i>Kretzschmaria deusta</i>	CBS 163.93	Germany	KC477237	KY610458	KY624227	KX271251	[10,54]
<i>Nemania bipapillata</i>	HAST 90080610	Taiwan	GU292818	N/A	GQ844771	GQ470221	[31]
<i>Nemania delonicis</i>	MFLU 19-2124	Thailand	MW240613	MW240542	MW342617	MW775574	[59]
<i>Nemania primolutea</i>	HAST 91102001 HT	Taiwan	EF026121	N/A	GQ844767	EF025607	[31]
<i>Obolarina dryophila</i>	MUCL 49882	France	GQ428316	GQ428316	KY624284	GQ428322	[10,60]
<i>Podosordaria muli</i>	WSP 167 HT	Mexico	GU324761	N/A	GQ853038	GQ844839	[31]
<i>Podosordariasp.</i>	CNF 2/11073	Croatia	OQ865223	OQ865228	OQ877111	OQ877122	This study
<i>Poronia punctata</i>	CBS 656.78 HT	Australia	KT281904	KY610496	KY624278	KX271281	[10,61]
<i>Pyrenopolyporus hunteri</i>	MUCL 52673 ET	Ivory Coast	KY610421	KY610472	KY624309	KU159530	[10,32]
<i>Pyrenopolyporus laminosus</i>	MUCL 53305 HT	France	KC968934	KY610485	KY624303	KC977292	[10,33]
<i>Pyrenopolyporus nicaraguensis</i>	CBS 117739	Burkina Faso	AM749922	KY610489	KY624307	KC977272	[10,33,36]
<i>Pyriformiascoma trilobatum</i>	MFLUCC 14-0012 HT	Italy	KP297402	KP340543	KP340530	KP406613	[34]
<i>Rhopalostroma angolense</i>	CBS 126414	Ivory Coast	KY610420	KY610459	KY624228	KX271277	[10]
<i>Rosellinia aquila</i>	MUCL 51703	France	KY610392	KY610460	KY624285	KX271253	[10]
<i>Rosellinia corticium</i>	MUCL 51693	France	KY610393	KY610461	KY624229	KX271254	[10]
<i>Rosellinia necatrix</i>	CBS 349.36	Argentina	AY909001	KF719204	KY624275	KY624310	[10,62]
<i>Rostrohypoxylon terebratum</i>	JF-TH 06-04 HT	Thailand	DQ631943	DQ840069	DQ631954	DQ840097	[63]
<i>Ruwenzoria pseudoannulata</i>	MUCL 51394 HT	D. R. Congo	KY610406	KY610494	KY624286	KX271278	[10]
<i>Sarcoxydon compunctum</i>	CBS 359.61	South Africa	KT281903	KY610462	KY624230	KX271255	[10,61]
<i>Stilbohypoxylon elaeicola</i>	YMJ 173	France	EF026148	N/A	GQ844826	EF025616	[31]
<i>Stilbohypoxylon quisquiliarum</i>	YMJ 172	France	EF026119	N/A	GQ853020	EF025605	[31]
<i>Thamnomycetes dendroidea</i>	CBS 123578 HT	France	FN428831	KY610467	KY624232	KY624313	[10,64]
<i>Xylaria bambusicola</i>	WSP 205 HT	Taiwan	EF026123	N/A	GQ844802	AY951762	[31]
<i>Xylaria brunneovinosa</i>	HAST 720 HT	France	EU179862	N/A	GQ853023	GQ502706	[31,65]
<i>Xylaria discolor</i>	HAST 131023 ET	USA	JQ087405	N/A	JQ087411	JQ087414	[66]
<i>Xylaria hypoxylon</i>	CBS 122620 ET	Sweden	KY610407	KY610495	KY624231	KX271279	[10,67]
<i>Xylaria multiplex</i>	HAST 580	France	GU300098	N/A	GQ844814	GQ487705	[31]
<i>Xylaria polymorpha</i>	MUCL 49884	France	KY610408	KY610464	KY624288	KX271280	[10]
<i>Xylaria sicula</i>	CNF 2/11087	Croatia	OQ865227	OQ865230	OQ877112	OQ877123	This study

3. Results

3.1. Molecular Phylogenetic Analyses

In this study, a total of 44 DNA sequences (11 ITS, 11 LSU, 11 *rpb2*, 11 *β-tub*) belonging to 11 fungal strains from the CNF were newly generated. Of the 11 fungal strains, four strains were identified as *E. cinnabarinum* (CNF 2/11046, 2/11047, 2/11052, 2/11053), two as *Hypoxylon croceoplum* Berk. & M.A. Curtis (CNF 2/11316, 2/11317) and one each as *E. liquescens* (CNF 2/11263), *Hypoxylon howeanum* Peck (CNF 2/11315), *Hypoxylon ticinense*

L.E. Petrini (CNF 2/11314), *Podosordaria* sp. (CNF 2/11073), and *Xylaria sicula* Pass. & Beltrani (CNF 2/11087). Associated accession numbers are marked in bold in Table 1.

The results of the phylogenetic analyses were similar to those previously published by Wendt et al. [10], Pourmoghaddam et al. [48], Song et al. [52] and Ma et al. [51]. Only significant branch support values of Bayesian posterior probability (BI-PP ≥ 0.95) and ultrafast bootstrap support (ML-BP $\geq 70\%$) are shown in the phylogram (Figure 1).

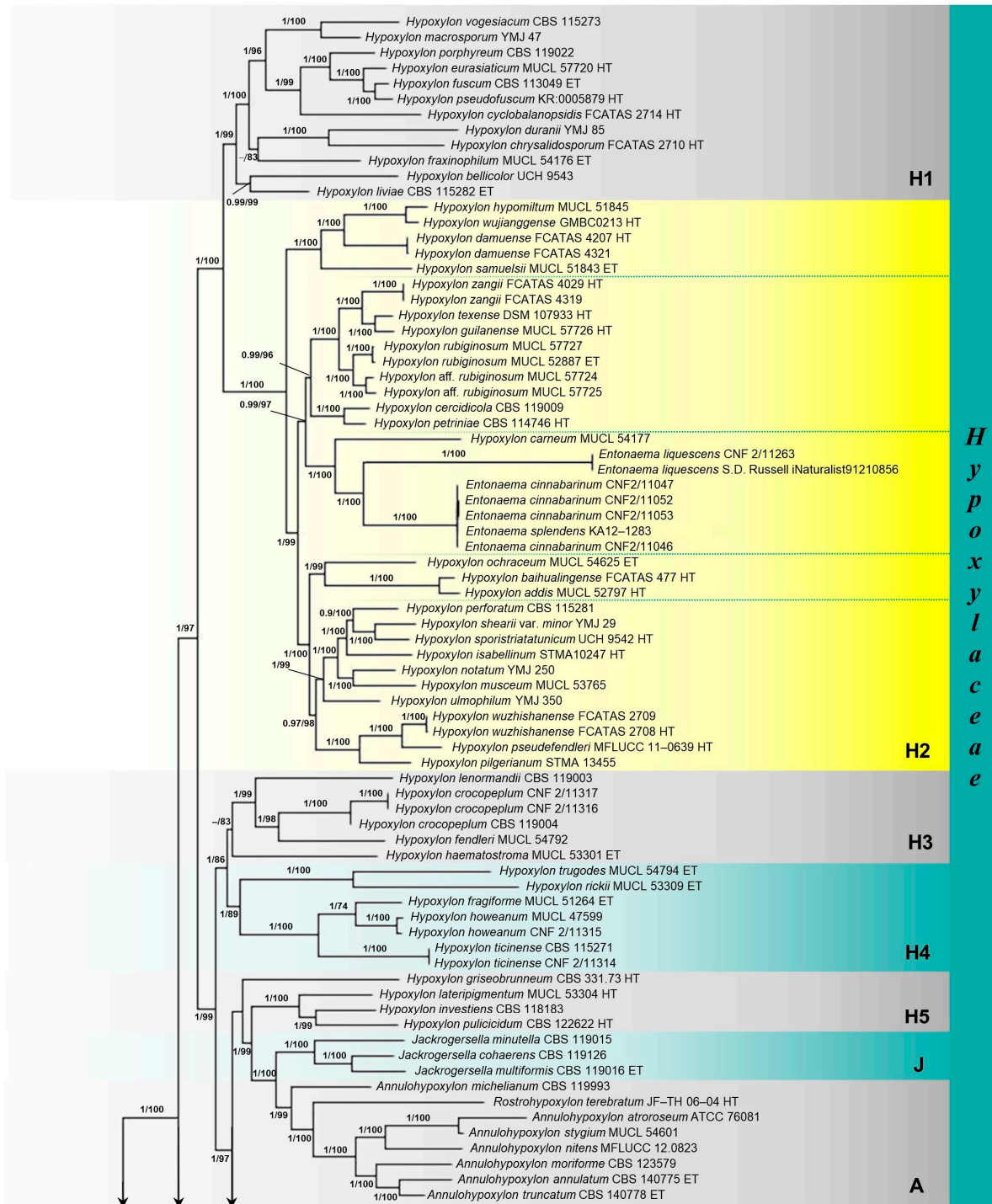


Figure 1. Cont.

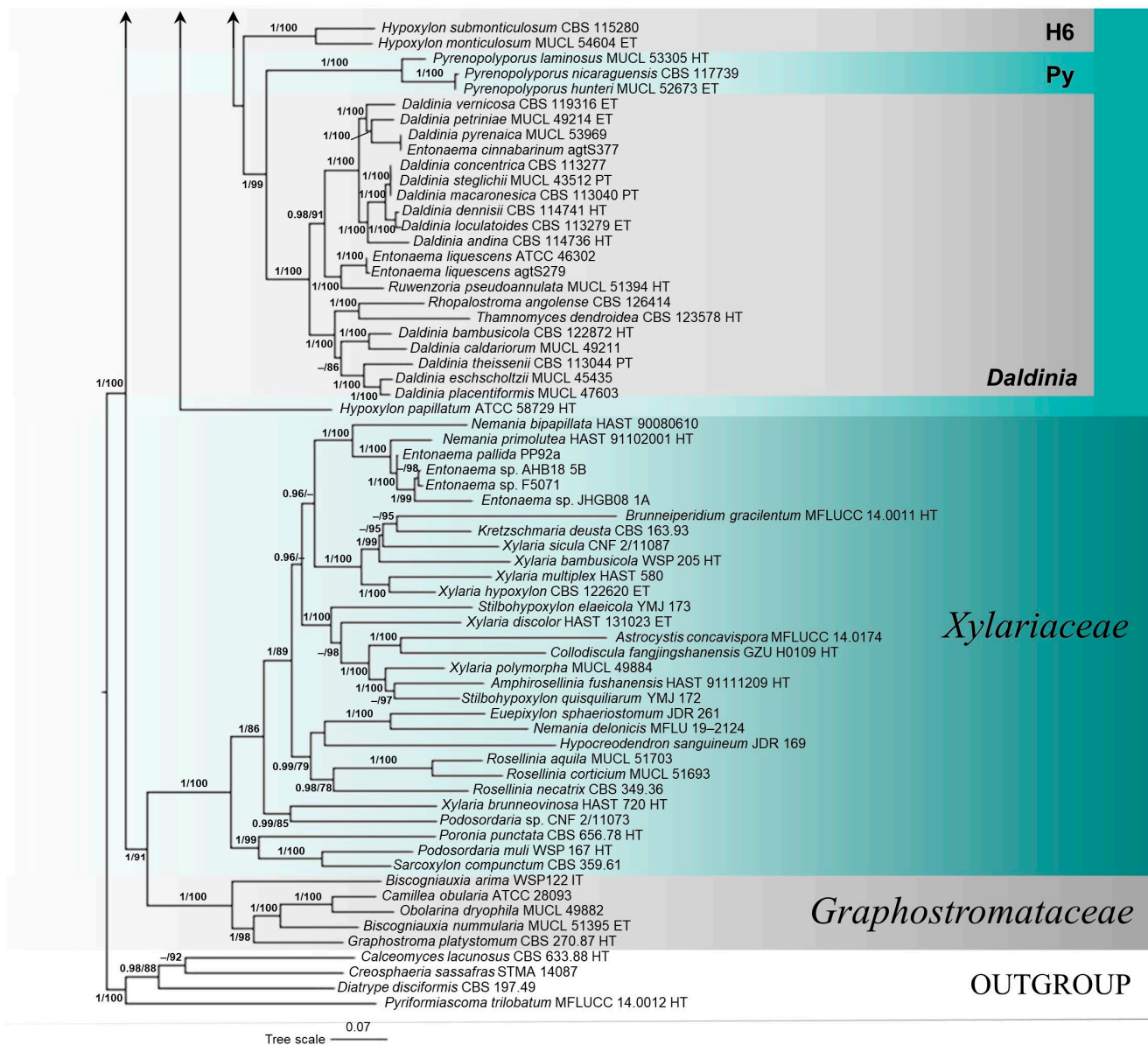


Figure 1. Phylogenetic tree of family *Hypoxylaceae*, based on Bayesian Inference (BI) and Maximum Likelihood (ML) analyses of concatenated four-gene (ITS, LSU, *rpb2*, *β-tub*) sequence alignment. Significant branch support values, Bayesian posterior probability (BI-PP ≥ 0.95) and ultrafast bootstrap support (ML-BP $\geq 70\%$), are presented at the nodes. Abbreviations: HT = holotype, ET = epitype, IT = isotype, PT = paratype.

The four-gene phylogeny revealed three main clades belonging to the families *Hypoxylaceae*, *Xylariaceae*, and *Graphostromataceae*. The most represented genus of *Hypoxylaceae* in the phylogenetic analysis was *Hypoxylon* Bull. with 76 strains, followed by 14 strains of *Daldinia* Ces. & De Not. and *Entonaema*, nine strains of *Annulohypoxylon* Y.M. Ju, J.D. Rogers & H.M. Hsieh, three strains of *Jackrogersella* L. Wendt, Kuhnert & M. Stadler, and *Pyrenopolyporus* Lloyd, and representative strains of *Rhopalostroma* D. Hawksw., *Thamnomycetes* Ehrenb., *Ruwenzoria* J. Fourn., M. Stadler, Læssøe & Decock, and *Rostrohypoxylon* J. Fourn. & M. Stadler. Phylogeny revealed paraphyly of the genus *Hypoxylon* (H1-H6) with the genera *Annulohypoxylon* (A), *Daldinia*, *Entonaema*, *Jackrogersella* (J), *Pyrenopolyporus* (Py), and *Rhopalostroma*, *Thamnomycetes*, and *Ruwenzoria* (*Daldinia* clade) embedded in the *Hypoxylaceae* clade.

The *Hypoxylon* H2 clade consisted of five strongly supported groups. Newly sequenced strains of *Entonaema* from the CNF, along with *E. splendens* KA12-1283 and *E. liquescens* S.D. Russell iNaturalist91210856, were phylogenetically very well differentiated (BI-PP = 1, ML-BP = 100) from a single lineage of *Hypoxylon carneum* Petch, in a strongly supported (BI-PP = 1, ML-BP = 100) subclade of the H2 clade. *Entonaema cinnabarinum* (CNF 2/11046, 2/11047, 2/11052, and 2/11053) clustered with *E. splendens* KA12-1283 and formed a maximally supported monophyletic clade (BI-PP = 1, ML-BP = 100) with *E. liquescens* CNF 2/11263 and the sister strain *E. liquescens* S.D. Russell iNaturalist91210856.

However, the *Entonaema* strains from the GenBank (with the exception of *E. splendens* KA12-1283) were distributed among other clades in the phylogenetic tree. In the *Daldinia* clade of *Hypoxylaceae*, *E. cinnabarinum* agtS377 recovered in a strongly supported monophyletic clade (BI-PP = 1, ML-BP = 100) with the epitype of *D. vernicosa* Ces. & De Not. (CBS 119316), the epitype of *D. petriniae* Y.M. Ju, J.D. Rogers & F. San Martín (MUCL 49214), and *D. pyrenaica* M. Stadler & Wollw. (MUCL 53969). Also, *E. liquescens* ATCC 4630 and *E. liquescens* agtS279 formed a monophyletic group (BI-PP = 1, ML-BP = 100) with *Ruwenzoria pseudoannulata* J. Fourn., M. Stadler, Læssøe & Decock (MUCL 51394) in the *Daldinia* clade. *Entonaema* sp. F5071, *E. pallida* PP92a, *Entonaema* sp. AHB18 5B, and *Entonaema* sp. JHGB08 1A were recovered in a phylogenetically fully supported clade (BI-PP = 1, ML-BP = 100) with the holotype strain of *Nemania primolutea* Y.M. Ju, H.M. Hsieh & J.D. Rogers (HAST 91102001) and *N. bipapillata* (Berk. & M.A. Curtis) Pouzar (HAST 90080610) in the *Xylariaceae* (Figure 1).

3.2. Taxonomy

Entonaema Möller, Bot. Mitt. Trop. 9: 306 (1901)

Generic diagnostic characters: Stromata pulvinate, subglobose to globose, often becoming irregularly lobed and/or wrinkled, especially at the tapered base, arising from woody substrates, most often from coarse woody debris. During the development, the enlarging cavity becoming filled with watery liquid. Stroma entonaematoid: stromatal flesh gelatinous without any concentric zonation, with ± vividly coloured surface until reaching late sporulation phase, when gradually turn to a horny or hard consistence and becoming wrinkled and carbonaceous due to the deposition of melanin pigments. Perithecia monostichous, developing immediately below bright coloured outer cortex. Interperithecial tissue ± carbonaceous at least around perithecial walls and in subperithecial layer (between perithecial bases and gelatinous inner fleshy layer). Ostioles inconspicuous, punctiform, umbilicate to papillate. Asci cylindrical with tapered base arising from croziers, apically with amyloid ring. Ascospores unicellular, walls with a shade of brown, with ± longitudinal ventral germ slit. Stromatal pigments of mitorubrin/rubiginosin type (azaphilones) are present in three species that are so far certain members of the genus confirmed either by phylogenetic (this paper) or HPLC analyses [2], viz. *E. liquescens* (type), *E. cinnabarinum*, and *E. globosum*. All three species also possess yellowish-orange to orange or rusty red extractable stromatal pigments and an indehiscent perispore in 10% KOH.

Anamorph: when cultivated, they often contain contamination, often of *Daldinia* spp., in need of thorough reinvestigation (see text below).

Notes: Three certain members of *Entonaema* (*E. liquescens*, *E. cinnabarinum* and *E. globosum*) differ from the most similar entonaematoid species from the genus *Xylaria* (*X. mesenterica*, *X. telfairii* (Berk.) Sacc. and allies) producing voluminous stromata with azonate and gelatinous to liquid interior, by orange to red KOH-extractable pigments vs. greenish-yellow ones, and by mitorubrin/rubiginosin-type metabolites, that lack in *Xylaria*. On the other hand, the three *Entonaema* spp. differ from the most phylogenetically related *Hypoxylon carneum* in having entonaematoid stromata with orange to red KOH-extractable pigments, while *H. carneum* has hypoxylloid, flat-pulvinate stromata with dark brown, thin (~200 µm thick), hard tissue below the perithecia and livid-violet KOH-extractable pigments, which are absent in aged material [48]. Contrary to *Entonaema* spp., azaphilone metabolites are not present in *H. carneum*.

Entonaema cinnabarinum (Cooke & Masee) Lloyd, Mycol. Writ. 7(69): 1203 (1923);
Figures 2–4 and 5J–L.

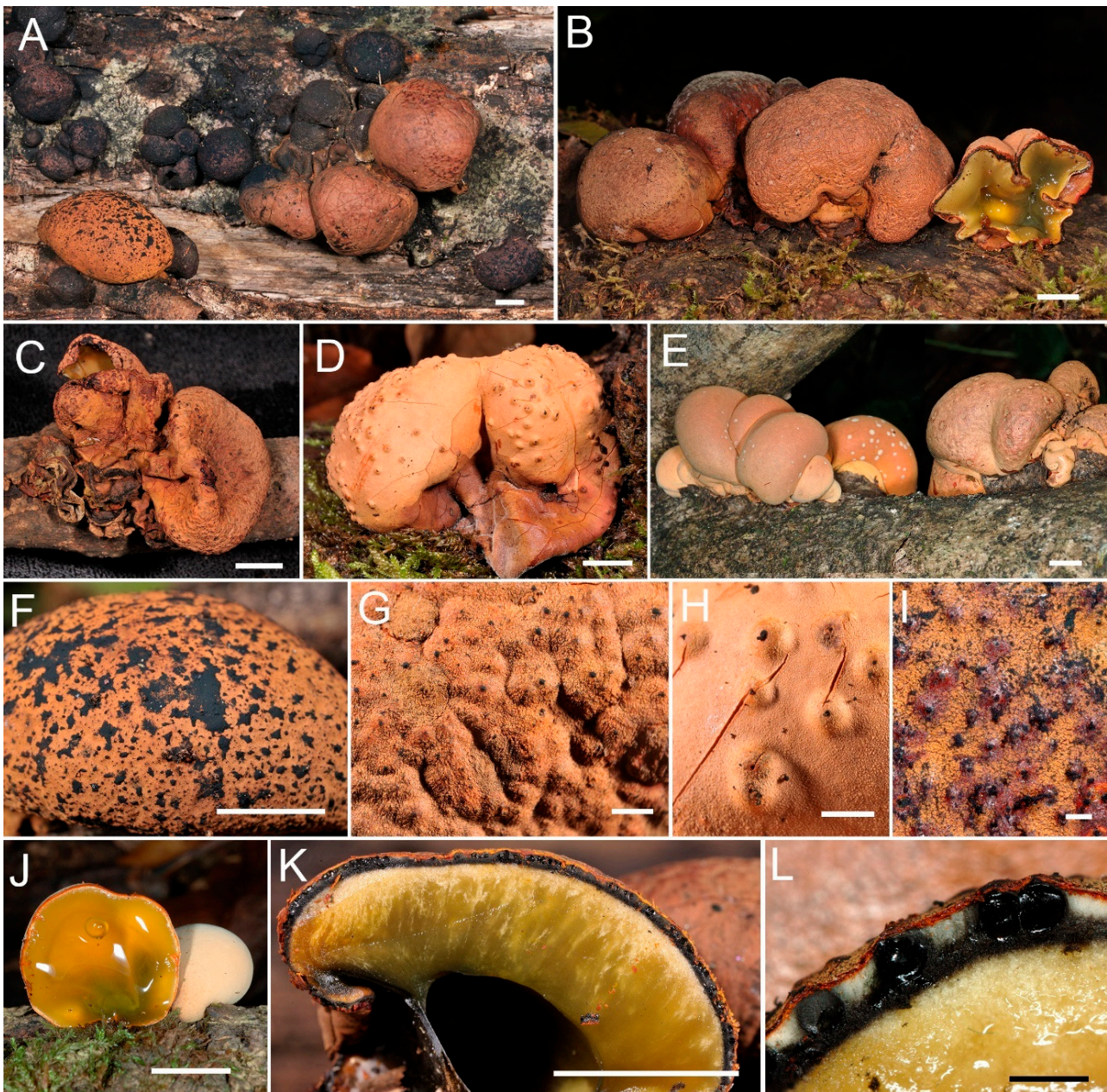


Figure 2. *Entonaema cinnabarinum*. (A) Stromata associated with *Daldinia childiae* J.D. Rogers & Y.M. Ju. (B–D) Mature stromata. (E) Young stromata. (F) Surface of the stroma dusted with ascospores. (G–I) Perithecial mounds with ostioles. (J) Section through young stroma. (K, L) Section through mature stroma. (A, F, G, K) CNF 2/11046; (B) (Croatia, 16.10.2021., no voucher); (C) CNF 2/11047; (D, H) CNF 2/11052; (E, J) (Croatia, 20.9.2009., no voucher); (I, L) CNF 2/8250. Bars: (A–F, J, K) = 1 cm; (G–I, L) = 1 mm. Photo: N. Matočec & I. Kušan.

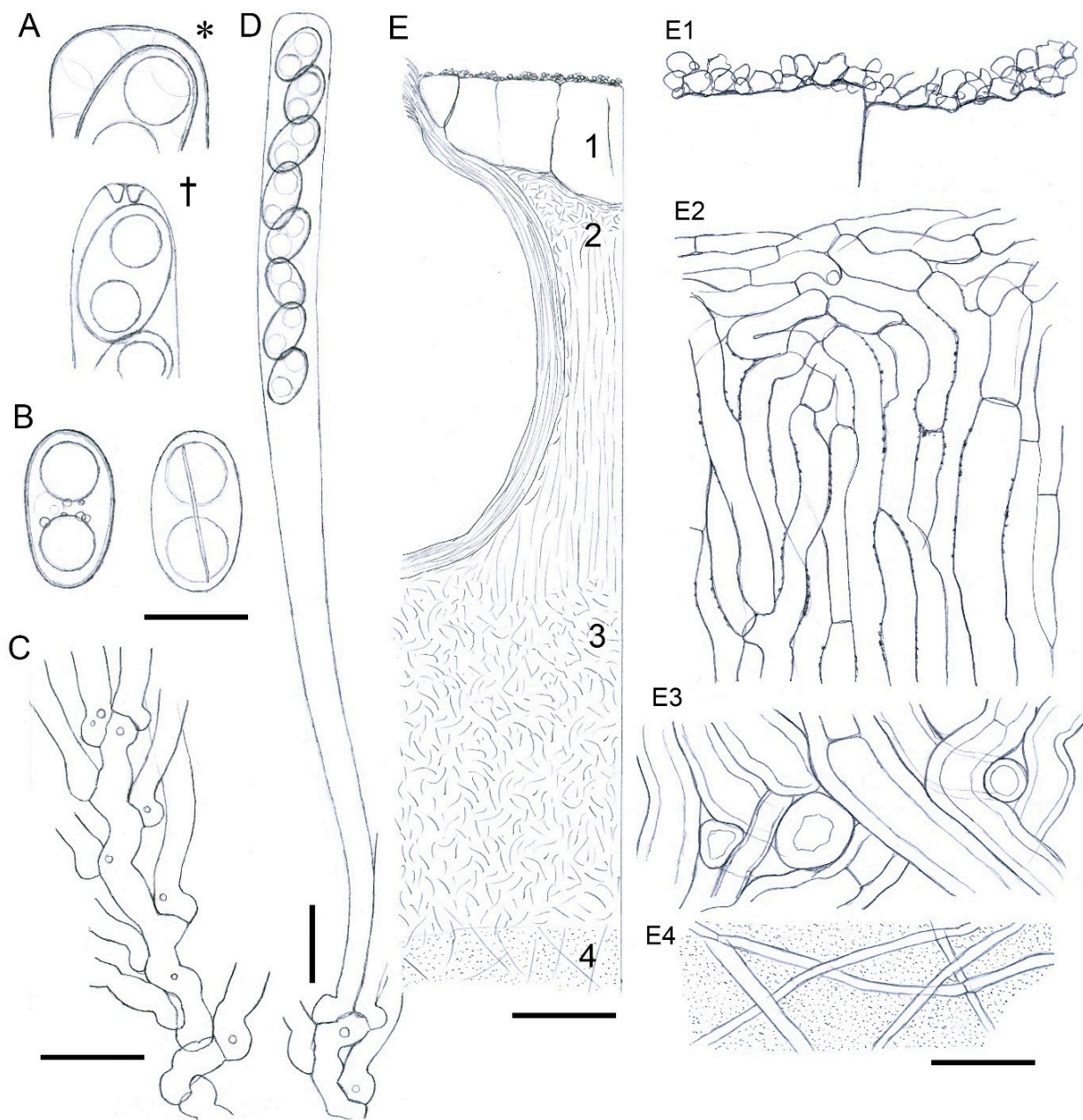


Figure 3. *Entonaema cinnabarinum* (CNF 2/8250). (A) Living (*) and dead (+) ascical apices. (B) Ascospores in frontal and dorsiventral view with a visible germ slit. (C) Ascogenous system. (D) Ascus. (E) Stromatal section ((E1) stromatal surface, (E2) interperithecial tissue, (E3) lower part of subperithecial layer, (E4) internal tissue). Bars: (A,B) = 5 μm; (C,D,E1–E4) = 10 μm; (E) = 100 μm. Del. N. Matočec.

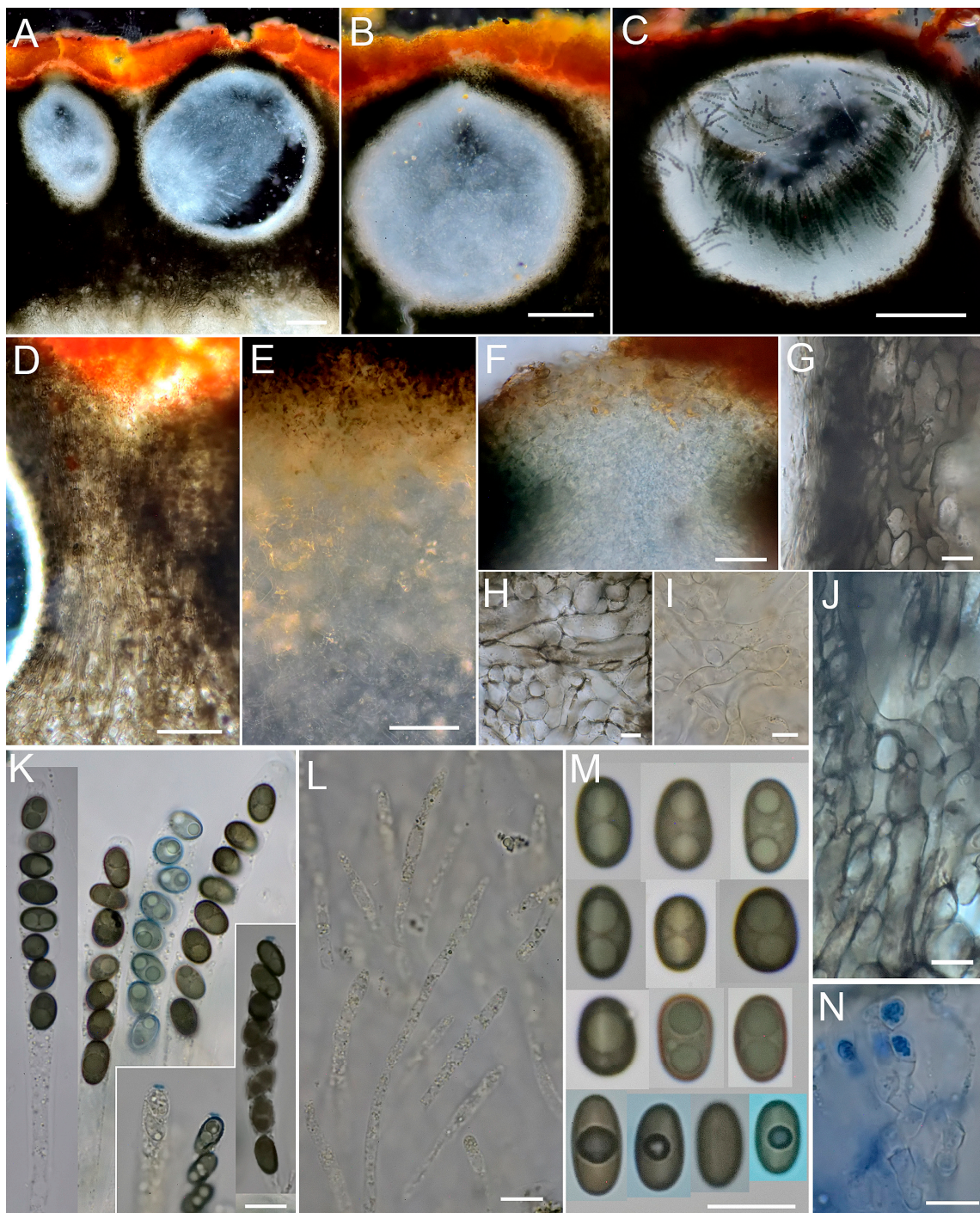


Figure 4. *Entonaema cinnabarinum*. (A–C) Sections through perithecia. (D) Interperithecial tissue. (E) Subperithecial layer (upper part) and internal tissue (lower part). (F) Ostiole. (G) Perithecial wall. (H) Cells of the subperithecial layer. (I) Cells of the internal tissue. (J) Cells in the interperithecial tissue. (K) Asci in H₂O and IKI. (L) Periphyses. (M). Ascospores in H₂O and CB (last row). (N) Croziers in CRB. (A,B,F,K–M) CNF 2/11046; (C,N) CNF 2/11047; (D,E,G–J) CNF 2/11053. Bars: (A–E) = 100 µm; (F) = 20 µm (G–N) = 10 µm. Photo: N. Matočec & I. Kušan.

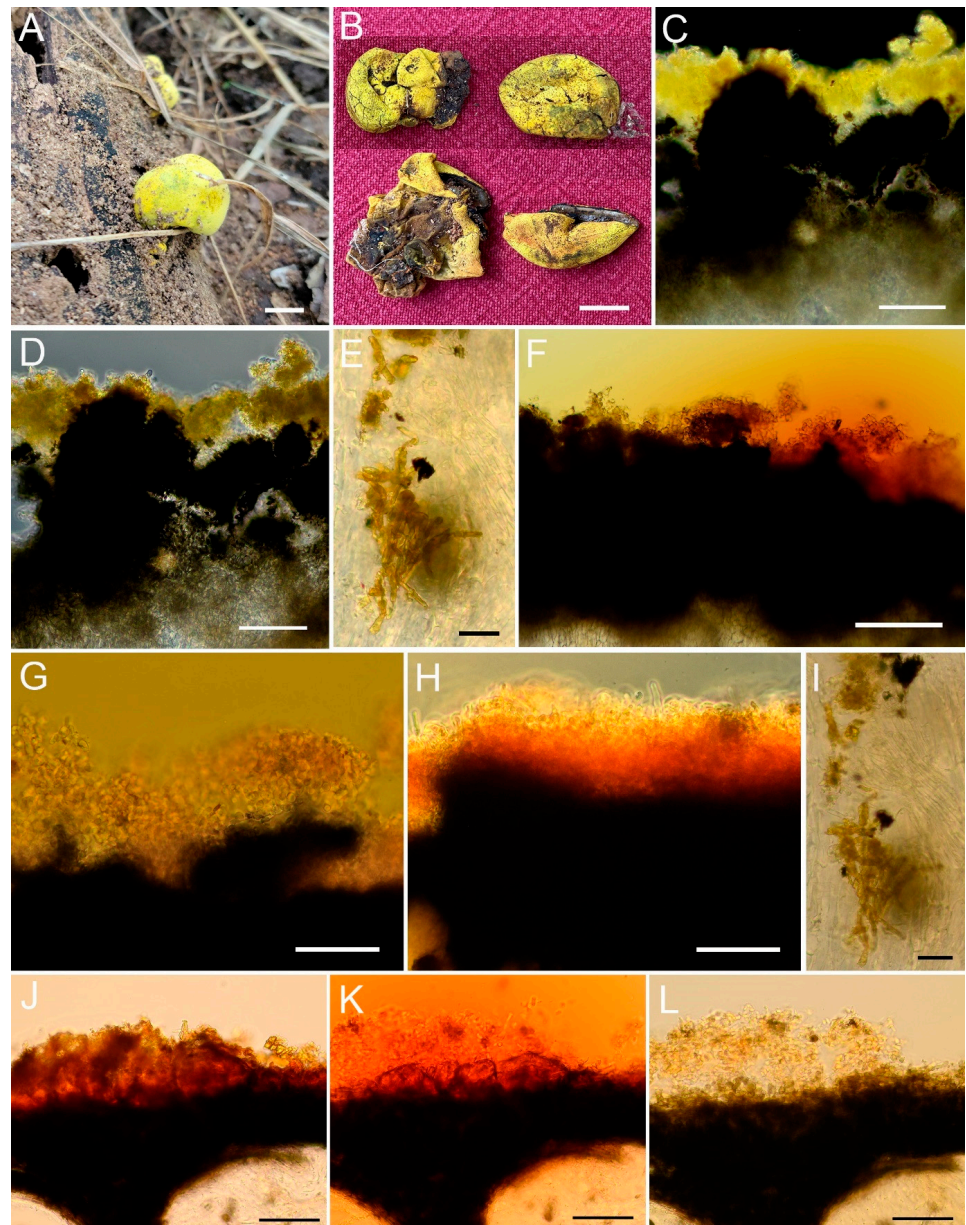


Figure 5. (A–I) *Entonaema liquescens* (CNF 2/11263), (J–L) *E. cinnabarinum* (CNF 2/11267). (A) Stromata *in situ*. (B) Stromata *ex situ*. (C,D) Lemon yellow pigments on the stromatal surface in H₂O (dark field, phase contrast). (E) Crystalloid pigments embedded inside interperithecial tissue (H₂O). (F) Pigment reaction upon adding 10% KOH. (G) Pigment soluble phase extracted in 10% KOH. (H) Pigment insoluble phase becoming rusty orange in 10% KOH. (I) Crystalloid pigments embedded inside interperithecial tissue in 10% KOH. (J) Rusty orange pigment granules on the stromatal surface in H₂O. (K) Pigment reaction upon adding 10% KOH. (L) Hyphal cover completely left without pigments after 10% KOH treatment. Bars: (A,B) = 1 cm; (C,D,F–H,J–L) = 50 μm; (E,I) = 10 μm. Photo: (A) T. Gonzales; (B) B. Bunyard; (C–L) N. Matočec & I. Kušan.

Basionym: *Xylaria cinnabarina* Cooke & Masee, *Grevillea* 15(76): 101 (1887)

= *Sarcoxyylon aurantiacum* Pat., *Bull. Soc. mycol. Fr.* 27(3): 331 (1911)

≡ *Entonaema aurantiacum* (Pat.) Lloyd, *Mycol. Writ.* 7(69): 1203 (1923)

Stromata: globose to irregularly convoluted, often constricted to the cerebriform at the base, *28–80 × 16–72 mm, when immature surface yellowish-cream to pale rosy, on smearing apricot orange, at maturity surface yellow-ochre to rosaceous-orange, fulvous, dull brick red, often cinnabar red around the ostioles, ostioles and some areas between

perithecia dusted blackish due to the ejected spores, with age becoming brownish-orange to reddish-brown, surface finely pruinose in younger stages, becoming smooth and often cracked with age. Ostioles punctate to papillate, rounded. Interior hollow and filled with pale yellow translucent viscose liquid; in section outer cortex orange to cinnabar red, 0.1–0.2 mm thick, covered with dull yellow detachable pruinose matter, beneath is a tough layer, 0.8–1 mm thick, composed of whitish to pale grey interperithecial tissue blackening with age, and a thin carbonaceous layer (in which perithecia are embedded) continuing to form a black layer underlying perithecial bases; perithecia globose to ellipsoid, black when mature; below the perithecial layer there is 2–6 mm thick, pale yellow to olivaceous, gelatinous, elastic, semitranslucent layer. In 5% and 10% KOH, the cortex is strongly brick red, liquid slightly discolouring, flesh apricot.

Ascomatal structures: Perithecia ranging from globose through ellipsoid to cylindrical, (350–)430–690 μm high, 340–660 μm wide, ostioles *95–120(–150) μm wide, periphyses hyaline eguttulate, cylindrical, apically obtusely tapered to sublanceolate, simple, one to few celled, flexuous, *2.5–5.2 μm wide. Asci cylindrical to narrowly clavate, 8-spored, $^{\dagger}100$ –136 \times 7.3–9 μm , *11.4–12.8 μm wide, delicate walled, wall persistent, not evanescent, apex thin-walled, apical dome barely visible, when *mature subtruncate-obtuse, † rounded to obtuse tapered, in IKI moderately (2bb) euamyloid, reaction zone simple, 2–2.4 μm wide, 1–1.2 μm high, ascoplasm highly vacuolate in all developmental phases, arising from Xylaria-type croziers, cells with weakly refractive globules. Ascospores brownish-olive to brownish-grey, dorsiventrally almost radially symmetrical, in profile slightly inequilateral, ellipsoid to suboblong with blunt ends, 1-celled, (8.1–)8.5–9.8–11.5(–12.1) \times (4.7–)5–5.9–6.8(–7.1) μm , Q = (1.34–)1.38–1.73–2.02(–2.16), (1)2(3)-guttulate, without sheath, germ slit ventral, longitudinal to \pm oblique and almost straight, 2/3 to almost whole spore length, spore wall thin, ± 0.2 μm thick, sporoplasm contain a deBary bubble in CB, perispore smooth, in 10% KOH indehiscent.

Stromatal tissue: Cortex (crust) covered with rusty red granules, mainly consisting of \pm homogenous block of highly refractive resin-like 50–210 μm thick layer, interspersed with locally densely set, hyaline, thin-walled sparingly septate cylindrical sinuous hyphae with blunt apices, hyphae $^{\dagger}2.4$ –6.5 μm wide. Interperithecial tissue *440–720 μm thick, mainly composed of vertically oriented *textura prismatica* with \pm thin-walled cells encrusted with very fine minute blackish granules, cells *3–7.7 μm wide, walls 0.3–0.5 μm thick. Perithecial walls ca. *50–80 μm thick, mainly composed of *textura angularis-prismatica*, walls of the same type as in interperithecial tissue, cells *7.5–16.1 \times 2.9–9.5 μm wide. Interperithecial tissue below perithecia gradually turn into subperithecial layer, 190–380 μm thick, which is composed of *textura fascicularis-intricata*, cells *7.5–16.5 μm wide, walls thickened and highly melanised, and a thin layer of *textura oblita* with intricate cell organization, cells *3.3–11 μm wide, walls hyaline, moderately refractive, gelified, up to 2.6 μm thick. Internal tissue of *textura gelatinosa*, hyphae widely spaced, hyaline, thin-walled, delicate, cells *3–8.8 μm wide, interspersed with rich gel.

Anamorph: not obtained on PDA, MEA, and OA.

Material examined:

CROATIA. Zagreb County: Malinje forest, Crna Mlaka near Jastrebarsko, 109 m a.s.l., 45.606817° N, 15.71695° E, on the lying trunk of *Quercus robur* in an old growth forest of *Q. robur*, *Fraxinus angustifolia*, *Ulmus minor*, *Carpinus betulus*, *Tilia* sp., 5 July 2009, M. Čerkez (CNF 2/8250); *ibid.* 45.605918° N, 15.716523° E, on the fallen branch of *U. minor*, 20 September 2009, N. Matočec & M. Čerkez (no voucher), *ibid.* 45.608199° N, 15.715229° E, on the fallen thick branch of *Q. robur*, 29 October 2020, I. Kušan & N. Matočec (CNF 2/11052), *ibid.* 45.608048° N, 15.715265° E, on the fallen thick branch of *Q. robur*, 29 October 2020, I. Kušan & N. Matočec (CNF 2/11053). Sisak-Moslavina County: Lonjsko Polje Nature Park, Opeke area near Kraljeva Velika, 95 m a.s.l., 45.370119° N, 16.820806° E, on the fallen semi-decorticated thin branch of *C. betulus* in a forest of *Q. robur*, *F. angustifolia* and *C. betulus*, 3 October 2020, J. Marković (CNF 2/11046); *ibid.* 45.373779° N, 16.821250° E, on the lying trunk of *F. angustifolia*, 16 October 2021, I. Kušan & N. Matočec, (no voucher);

Trebeški dol area near Kraljeva Velika, 95 m a.s.l., 45.369202° N, 16.780788° E, on the fallen corticated thin branch of *Salix* sp. in a forest of *Q. robur*, *C. betulus* with *Salix* sp., 17 October 2020, M. Josipović, (CNF 2/11047); Tena's walking path near Ilova, 99 m a.s.l., 45.433639° N, 16.823863° E, on the lying trunk of *Fraxinus angustifolia* in an old growth forest of *Q. robur*, *F. angustifolia* and *Ulmus minor*, 28 September 2021, J. Marković, I. Kušan & N. Matočec, (CNF 2/11267). This species was here recorded for the first time for Croatia.

Entonaema liquescens Möller, Bot. Mitt. Trop. 9: 307 (1901); Figure 5A–I
 = *Xylaria splendens* Berk. & M.A. Curtis, J. Linn. Soc., Bot. 10(46): 382 (1868)
 ≡ *Entonaema splendens* (Berk. & M.A. Curtis) Lloyd, Mycol. Writ. (Cincinnati) 7(69): 1202 (1923)

≡ *Glaziella splendens* (Berk. & M.A. Curtis) Berk., in Glaziou, Vidensk. Meddel. Dansk Naturhist. Foren. Kjøbenhavn 80: 31 (1879)

NOTE: The studied collection of *E. liquescens* consisted of two stromata, both immature. Perithecia and ascus structures were found only in an immature stage, without any traces of developed ascospores. It was stromata globose to slightly cerebriform, 22–29 × 17–20 mm, lemon yellow, and hollow. Pigments on the stromatal surface were lemon yellow in H₂O (best visible in dark field, Figure 5C). After adding 5% KOH and 10% KOH, they extract a yellowish-orange to rusty orange colour to the medium, while the remaining pigments that are fixed in the cortex turn rusty orange (Figure 5H). The crystalloid pigments embedded in interperithecial tissue remain unchanged (Figure 5E,I). Since *E. liquescens* and *E. cinnabarinum* have very similar microscopical characters usually used in species distinctions, the two species differ sharply in their microchemical traits. In contrast to *E. liquescens*, *E. cinnabarinum* lacks an insoluble pigment phase whereby the cortical layer remains subhyaline after KOH treatment (Figure 5L). Additionally, the two species differ by the pigment granules colour in *H₂O, which is lemon yellow in *E. liquescens* (Figure 5C,D) and rusty red in *E. cinnabarinum* (Figure 5J).

Material examined: USA. Kansas: Morris Co., Council Grove Reservoir, on the fallen decorticated branch of a *Quercus* sp. in a forest of *Quercus stellata* and *Q. marilandica*, 18 September 2021, T. Gonzales, (CNF 2/11263).

Worldwide identification key to the putative species of *Entonaema*

- (1) Stromatal extractable pigments greenish yellow in 10% KOH, but red in NH₃ *Xylaria* p.p.
 - Stromatal extractable pigments orange to brick red or entirely absent in 10% KOH, orange in NH₃ *Entonaema* (2)
- (2) Stromatal orange to red pigment granules present in the section immediately beneath the stromatal surface and around the perithecial ostioles, stromatal extractable pigments in 10% KOH brick red 3
 - Stromatal pigment granules in the section of the stromatal cortex yellow, green, or absent, stromatal extractable pigments in 10% KOH yellowish-orange to orange, or absent 4
- (3) Stromatal pigment in the section immediately beneath the stromatal surface and around the perithecial ostioles rusty orange, ostioles papillate, perithecia 300–600 µm in diam., ascospores 9–13 µm long *E. cinnabarinum**
 - Stromatal pigment in the section immediately beneath the stromatal surface and around the perithecial ostioles blood red, ostioles umbilicate, perithecia 100–300 µm in diam., ascospores 8–10 µm long *E. globosum*
- (4) Stromatal surface with olivaceous tint in maturity, perithecia 200–500 µm in diam., ascospores cylindrical with ± blunt ends, 8–13 × 3.5–6.5 µm; stromatal extractable pigments orange in 10% KOH, but not tested in *E. siamensis* 5
 - Stromatal surface yellowish-tan or dark reddish-brown in maturity, perithecia 500–1000 µm in diam., ascospores ellipsoid with subacute ends, 13–18 × 6.5–8 µm, stromatal extractable pigments absent with 10% KOH 6
- (5) Stromatal pigment in the section immediately beneath the stromatal surface and around the perithecial ostioles vividly yellow, ascospores 5–6.5 µm wide, asci 6–10 µm wide *E. liquescens**
 - Stromatal pigment in the section immediately beneath the stromatal surface and around the perithecial ostioles consists of green granules, ascospores 3.5–5 µm wide, asci 5–6 µm wide *E. siamensis*
- (6) Stromatal surface dark reddish-brown, perithecial ostioles prominently papillate, ascospores up to 15 µm long *E. dengii*
 - Stromatal surface yellowish-tan with or without reddish-orange tinges, perithecial ostioles inconspicuous, punctate, ascospores always exceed 14.5 µm in length (up to 18 µm) 7
- (7) Ascospores lemon-shaped with ± papillate ends, perispore indehiscent in 10% KOH *E. moluccanum*
 - Ascospores ellipsoid with ± tapered ends, perispore dehiscent in 10% KOH *E. moluccanum*
 ss. Sánchez-Jácome & Guzmán-Dávalos

An asterisk (*) denotes species belonging to *Entonaema* confirmed by phylogenetic analysis.

3.3. Ecology and Biogeography

All scientific publications accessible to the authors and the GBIF database (an extensive high quality online database on worldwide occurrences of biological species; www.gbif.org, accessed on 26 June 2023) were searched for verifiable *Entonaema* records in an attempt to provide better understanding of the ecology and biogeography of *Entonaema* species. A detailed analysis of a total of the here-accepted 266 worldwide *Entonaema* records that were attributable to a species (209 finds of *E. liquescens*, 51 of *E. cinnabarinum*, two of *E. globosum*, one of each *E. dengii*, *E. mollucanum*, *E. 'mollucanum'*, and *E. siamensis*), accompanied with precise localities, revealed much more information on biogeographic traits on the two most frequent species (*E. liquescens* and *E. cinnabarinum*) than in any of the previous studies. According to all here-accepted records of *Entonaema* spp. with known record dates, two phenological fructification patterns were recognized: (a) Mature stromata may be found all year round in tropical rainforest zones (Af) or depending on rainy period in monsoon (Am) and savannah areas (Aw); and (b) immature stromata were found during May and June, and mature ones from July to October (November) in four-season warm temperate northern zones (Cfa, Cfb, Csa, Cwa), see Figure 6. In the areas under the warm temperate climatic regime, immature stromata may also be found during summer and the autumn along with the mature ones, and quite often the maturation of perithecia/asci may completely fail in certain years in some localities ([2,68], GBIF data, our study), or only a few perithecia manage to ripe per stroma. Consequently, this unpredictability posed difficulties when re-studying fungaria material. A number of valuable collections consist only of sterile stromata (cf. [2,4,5,69]). According to all accepted records accompanied either with ecological data (substrate, habitat) or precise geographic coordinates, *Entonaema* species were mainly found in various forest ecosystems (including managed ones), or sometimes in city parks, on widely diverse angiosperm tree hosts, very often on coarse woody debris. Nearly all records found in warm temperate areas were in the near vicinity of freshwater bodies (rivers, rivulets, creeks, lakes, etc.).

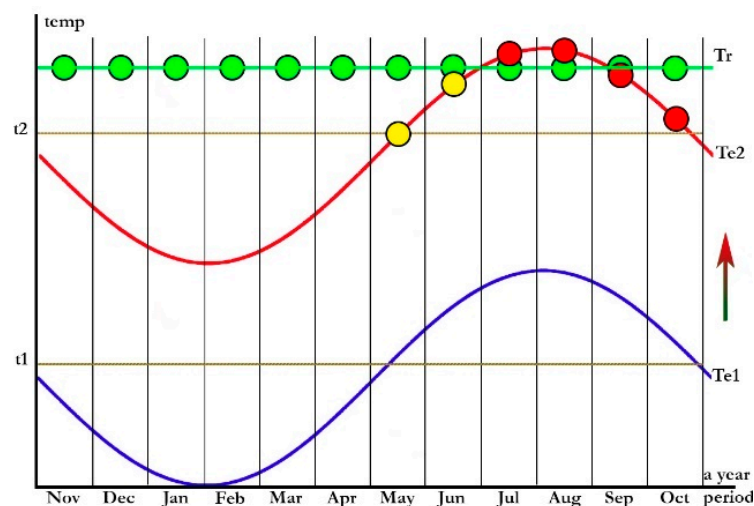


Figure 6. Two *Entonaema* fructification patterns: tropical pattern (Tr) represented by green circles as potential records of ripe stromata during all year (Af climate type) or depending on rainy season (Aw and Am climate types); warm temperate zone pattern (Te2) represented by yellow circles corresponding to immature stromata and red circles to ripe stromata, that occur during the warmest months. Areas with cool temperate climate (Te1) are devoid of *Entonaema* records. Legend: t1 = cardinal minimum temperature that would enable ascospore overwintering; t2 = minimal temperature needed for stromatic development; right arrow denotes climatic shift from Dfa (cool temperate climatic type) to Cfa (warm temperate climatic type).

According to 266 records accepted by us, *E. liquescens* is by far the most-frequently recorded species (209 records). This species has transcontinental distribution in humid tropical (Am and Aw) areas of Africa (Kenya, Mayotte Island, South Africa, Uganda—[3,5], Zaire—[5]), the Americas (Brazil, Colombia—[4], Costa Rica, Cuba—[3], El Salvador, Honduras, Mexico—[5], Panama—[2], Trinidad and Tobago, Venezuela), Asia (China—[5], Thailand—[13]), and in humid warm temperate (Cfa, Cfb, Csa, Cwa) areas of Asia (India, Japan—[3]) and the Americas (Argentina—[5], Brazil—[1,2,5], Ecuador, Mexico, USA—[5,70]). There are also a few records of this species in cool temperate areas near the edge of the areas of warm temperate climatic regimes: the Russian Far East (Dwb) and northern USA (Dfa).

Entonaema cinnabarinum is another relatively frequently recorded species, with 51 records accepted here. This species also has transcontinental distribution in humid tropical (Af and Am) areas of Africa (Congo—[5], Sierra Leone, Uganda—[5]), the Americas (Costa Rica—[5]), Asia (India—[3], Philippines—[70], Sri Lanka—[3]), Oceania (Australia—[11], Nova Caledonia—[71]), and in humid warm temperate (Cfa, Csa, Cwa, Cwb) areas of Asia (Iran—[2], Japan—[70], Nepal), the Americas (Mexico—[2], USA), and Europe (Bulgaria—[72], Croatia—this paper, France—[2], Hungary—[68], Russia—[73], Serbia, Spain). There are also a few records of this species in cool temperate regions near the edge of the areas of warm temperate climatic regimes: the Russian Far East (Dwb—[74,75]).

This study did not bring any new distributional or taxonomic data for other species, because all records are already treated in earlier publications. The following four species are apparently so far confined to a tropical climatic areas. *Entonaema globosum* is so far known only from two Mexican localities under the influence of tropical rainforest (Af) and savannah (Aw) climatic regimes [12,69]. *Entonaema siamensis* is apparently known only from a type locality in Thailand [13], while *E. dengii* is from a type locality on Hainan Island, China [5], both situated in the areas of tropical savannah climate (Aw). *Entonaema moluccanum* is known only from a type locality on Halmahera Island, Indonesia [5], under influence of a tropical rainforest climate (Af). We agree with Stadler et al. [2] that, according to perispore dehiscence and different ascospore morphology, material published by Sánchez-Jácome and Guzmán-Dávalos [76] does not represent *E. moluccanum*, but some undescribed species. Also, it is hitherto known from a single locality under a warm temperate climatic regime (Cwa), outside of tropics. The first record from each locality in published papers are cited above. The other country records were mainly covered solely by GBIF.

4. Discussion

4.1. Taxonomic Implications

A data matrix for DNA sequence alignment was constructed to re-analyse the phylogenetic position of three entonaemoid species, viz. *E. liquescens*—a type species, *E. cinnabarinum*, and *Xylaria mesenterica* (Möller) M. Stadler, Læssøe & J. Fourn.—a former member of *Entonaema* (= *E. mesentericum* Möller, *E. pallidum* G.W. Martin). With the emphasis on a wide selection of hypoxylid species groups previous chemotaxonomic research revealed that three *Entonaema* species (*E. liquescens*, *E. cinnabarinum*, and *E. globosum*) share the same stromatic HPLC profiles [2], i.e., mitorubins and rubiginosins (group of azaphilone metabolites), that are characteristic to members of *Hypoxylaceae*, but not to *Xylariaceae*. Consequently, we included a wide spectrum of hypoxylid species in our phylogenetic analysis. The sequences of *E. liquescens* and *E. cinnabarinum* obtained from perithecial elements were newly generated for that matter. In the previous studies [10,48,51], the ITS-LSU-*rpb2*- β -*tub* phylogeny confirmed *Hypoxylon* as a paraphyletic genus in the *Hypoxylaceae* that was recovered in at least six independent clades. Only one *Entonaema* strain (*E. liquescens* ATCC46302, [10]) was included in the study and was placed between the two *Daldinia* clades as a sister species to *Ruwendoria pseudoannulata* MUCL 51394. *Hypoxylon carneum* was recovered as a single lineage with *H. cercidicola* (Berk. & M.A. Curtis ex Peck) Y.M. Ju & J.D. Rogers, *H. petriniae* M. Stadler & J. Fourn., and *H. rubiginosum* (Pers.) Fr. as the phylogenetically closest species, but distant from the type species *H. fragiforme* (Pers.) J. Kickx f.

In the present study, the phylogeny based on concatenated analysis of ITS, LSU, *rpb2* and *β-tub* gene regions supported previous studies, but nested two analysed species, *E. liquescens* and *E. cinnabarinum*, in the H2 subclade of *Hypoxylaceae*, next to *H. carneum* as a sister lineage and distant from the strain *E. liquescens* ATCC46302 in the *Daldinia* clade. On the chemotaxonomic level, *H. carneum* differs from *Entonaema* species in non-azaphilone metabolites (carneic acids) that accumulate in the stromata [77,78]. Additionally, *H. carneum* differs from true *Entonaema* spp. (*E. liquescens*, *E. cinnabarinum*, and *E. globosum*) in flat-pulvinate stromata with only very thin, hard, dark brown tissue below the perithecia and livid-violet KOH-extractable pigments, which are absent in aged material (see Section 3.2 above). Moreover, in addition to the CNF collections of *Entonaema*, nine other *Entonaema* strains were phylogenetically analysed in this study. Two strains (*E. liquescens* S.D. Russell iNaturalist91210856 [41] and *E. splendens* KA12-1283) were recovered with CNF collections in the H2 subclade of *Hypoxylaceae* as ‘true’ *Entonaema*. The phylogenetic placement of *E. pallidum* in the *Xylariaceae* in our study supports the research of Stadler et al. [2], who recognised similarities between *E. pallidum* and *Xylaria* spp. in their morphology, 5.8S/ITS nrDNA sequences, and HPLC profiles. Strains named *Entonaema* sp. JHGB08 1A, *Entonaema* sp. AHB18 5B [43], and *Entonaema* sp. [44] recovered alongside *E. pallidum* in the *Xylaria* clade, and consequently cannot be considered members of *Entonaema*. Therefore, our phylogenetic results agree with Lücking et al. [79] that comparison of sequences with GenBank blastn alone [42–44] is insufficient for accurate taxonomic characterisation because the reference databases used for molecular identifications are still incomplete and often contain erroneously named sequences. Furthermore, in our opinion only the integrative approach is acceptable if we seek for stabilised and operable taxonomy [80].

Our phylogenetic placement of true *Entonaema* spp., viz. the type species *E. liquescens* and *E. cinnabarinum* in *Hypoxylaceae*, and on the other hand ‘*Entonaema*’ *pallidum* in *Xylariaceae* is now in correlation with earlier stromatal chemotaxonomic characterisation of the two separate groups, where *E. liquescens* and *E. cinnabarinum* have mitorubrinoid/rubiginosinoid HPLC profiles, characteristic for *Hypoxylaceae*, whereas ‘*Entonaema*’ *pallidum* possesses xylaralic HPLC profile characteristic for *Xylariaceae* [2]. Clear overlapping of genetic and phenetic traits in a small *Entonaema* clade led us to retain its current generic concept, which would contain only several species around *E. liquescens* characterised by vividly coloured, large, vesiculose hollow stroma with elastic gelatinous flesh that contain liquid matter inside its cavity, possessing yellow, orange to red stromatic KOH extractable pigments, and mitorubrine/rubiginosine HPLC profile. This would necessitate the erection of several more small genera inside the H2 clade of *Hypoxylon* s.l. [10]. In such a concept, only a few species would thus clearly belong to *Entonaema*, viz. *E. liquescens* (type), *E. cinnabarinum*, and, relying on specific morphological–chemotaxonomical traits, also *E. globosum* and *E. moluccanum* ss. Sánchez-Jácome & Guzmán-Dávalos. The true affinity of *E. dengii*, *E. moluccanum* ss. str., and *E. siamensis* is yet to be ascertained.

4.2. Molecular Misinterpretations

The strains *E. liquescens* ATCC46302 [10,15], *E. liquescens* agtS279 [14], and *E. cinnabarinum* agtS377 [14] were recovered in the *Daldinia* clade of *Hypoxylaceae*, similar to previous studies [10,14,48,51]. The phylogenetic position of *Entonaema* in the *Daldinia* clade based on the ITS region was not well supported [14], but maximally supported when the phylogeny was based on four gene regions (including protein gene regions), as presented by Wendt et al. [10] and Wibberg et al. [15]. In these studies, *Entonaema* species were not described by thorough macro- and micromorphological examination of fruiting bodies, or by chemotaxonomical characterization, and DNA for sequencing was obtained from culture collections. The close phylogenetic relationship of *Entonaema* and *Daldinia* species was supported by the naphthalene and chromone derivatives produced by both [70]. On the other hand, the presence of mitorubrin-type azaphilones in the ascospores of *E. cinnabarinum* and *E. liquescens* [70] and the absence of binaphthalenes (which are ubiquitous in *Daldinia*) [2] clearly distinguishes *Entonaema* from *Daldinia* at the chemotaxonomic level.

Our *Entonaema* finds were often associated with *Daldinia* spp. (Figure 2A), including *D. childiae*, whose stromata have been found on the same dead wood fragments together with the stromata of *E. cinnabarinum* (cf. [38]). All our efforts to establish *E. cinnabarinum* in axenic culture failed, where freshly ejected ascospores did not germinate on any of the three tested nutrient media (PDA, MEA and OA), regardless of the varied procedure. In cases where stromata of *Entonaema* were dusted by spores originated from neighbouring *Daldinia* stromata, the agar plates were occupied by rapid mycelial growth and conidial development of *Daldinia* contamination. It seems that *Daldinia* may often take over the plates because *E. cinnabarinum* is hardly culturable, if at all, while *Daldinia* propagules germinate very rapidly and its mycelia are very fast growing. Therefore, it is not surprising that the same happened with two critical attempts to obtain culture of *E. liquescens*—ATCC 46302 strain, KANSAS, USA [6], and of *E. cinnabarinum*—CBS 113034, Pyrénées Atlantiques, FRANCE [14,70] in previous *Entonaema* studies. As a consequence, all sequences derived from this reference cultures actually belong to some *Daldinia* species, but not to *Entonaema* (*E. liquescens* nor *E. cinnabarina*), what Wibberg et al. [15] already justifiably suspected for *E. liquescens*. This further led to erroneous molecular identification of *E. cinnabarinum* in the study of symbiotic relationships between saproxylic *Xiphydria* wasps and fungi from the genera *Daldinia* and *Entonaema* [81], which turned out to be true only for the fungi of the former genus (cf. [38]). Consequently, the anamorph of *Entonaema* itself remains vague.

4.3. Distribution and Biogeography

Outside America's tropical areas, *E. liquescens* was, until the 1980s, known only from the most southeastern USA with its very humid and warm temperate climate (Cfa), starting with Florida—1939, Louisiana—1956, Alabama—1965, Georgia—1978, and Mississippi—1986 (Figure 7), including few finds in the warmest areas of Kansas along the Missouri River (1979). The species was not found in northern states on the verge of the Cfa climatic area and cooler temperate climatic area (Dfa) (Nebraska, Indiana, Ohio, and Iowa), as well as inside the Dfa area before 2016. Since this time, *E. liquescens* occurrences in those northern areas has become quite regular—as much as in the southern states—and spreading along the watercourses of the Mississippi, Missouri, Kansas, Platte, Illinois, Ohio, and Tennessee rivers, and their tributaries, as well as along the warm Atlantic Coast and the Potomac River (cf. www.gbif.org, accessed on 26 June 2023).

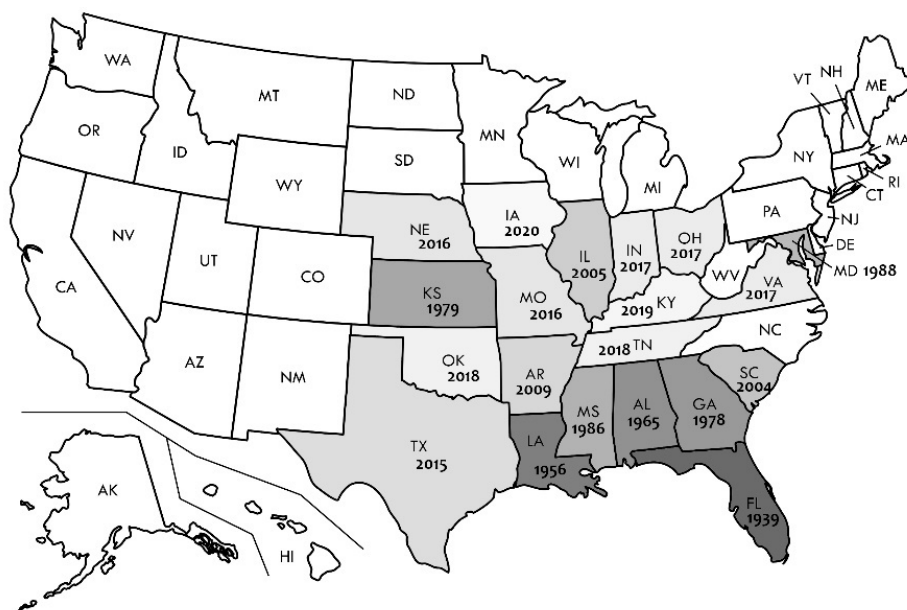


Figure 7. Map of USA with year of first record of *Entonaema liquescens* per federal state. Shading intensity reflects the time order in records, where the darkest shade represents the oldest known record.

Virtually all precisely recorded localities revealed (with the aid of Google Earth Pro) that the species' habitats are either flood plains or alluvial forests, developed along the watercourses, at lake banks, or under the dams of hydroaccumulation reservoirs. The species is mostly distributed in the area of the warm temperate Cfa climate type [30], especially in the USA and Japan. *Entonaema liquescens* is not known in Europe so far.

Apart from a single Bulgarian longose forest (Mediterranean flood alluvial forest) [72,82], the presence of *E. cinnabarinum* in Europe (being one of the best explored areas in general, in mycological terms) is recorded only from the turn of the 21st century onwards [68,70,73,83]. Longoses represent subtropical oases in the otherwise relatively dry Mediterranean, and in temperate zones in general, because soil humidity is much prolonged by canopy coverage and by riverine inundation, and therefore not entirely dependent on precipitation. On the other hand, the habitat's ground substrates are well protected from heavy frosts and dry freezing under dense canopy coverage and thermic marine influence. Therefore, knowing the thermophilic species' preference, we could assume that this species might have been inhabiting such habitat types long before it was first recorded in 1987 in Bulgaria. Outside Bulgarian longose, the species was first found in the warm temperate area of the Pyrénées Atlantiques in France (1999), then in the Asturian rivulet valley of Spain (2006), Sochi in Russian Federation (2011), and with repetitive records in the Pannonian Plain in Croatia (since 2009), Hungary (2018), and Serbia (2022), see Figure 8.

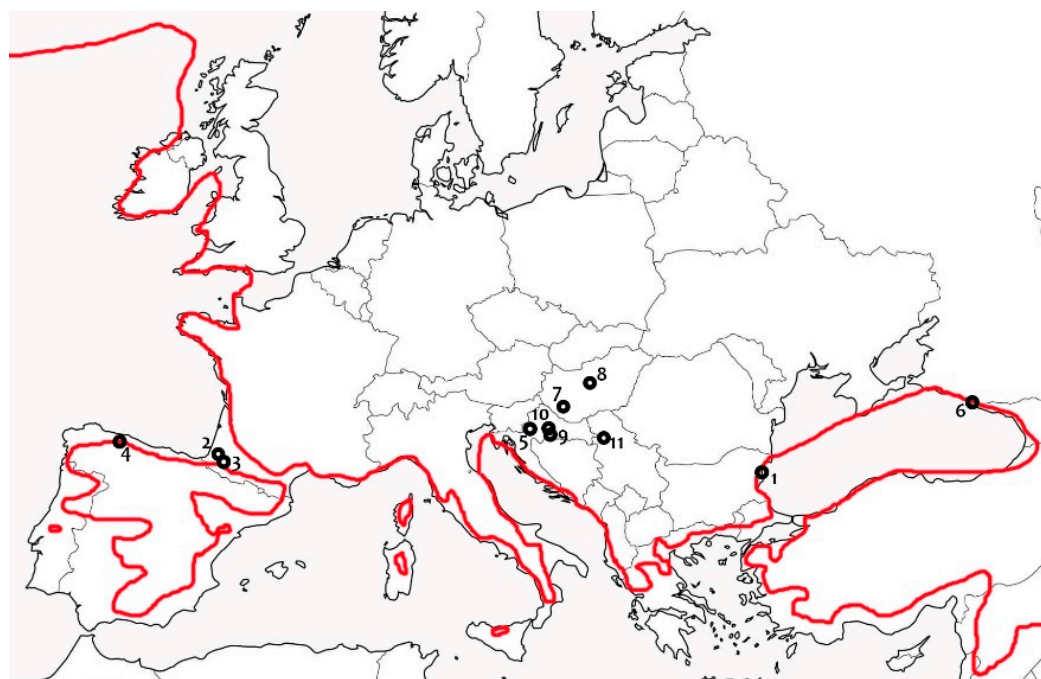


Figure 8. Known localities of *Entonaema cinnabarinum* in Europe, arranged according to the year of first record: 1—Kamchiya longose, Bulgaria (1987), 2—Auterrive and 3—Oloron-Ste. Marie, both Pyrénées Atlantiques, France (1999), 4—Belmonte, Asturias, Spain (2006), 5—Crna Mlaka, Zagreb County, Croatia (2009), 6—Agurskye waterfalls near Sochi, Russian Federation (2011), 7—Tókaj forest park, near Kaposvár, Hungary (2018), 8—Selyemrét Nature Trail, Ócsa, Pest County, Hungary (2019), 9—Opeke area near Kraljeva Velika, Sisak-Moslavina County, Croatia (2020), 10—Piljenice area near Ilova, Sisak-Moslavina County, Croatia (2021), and 11—north from Divoš, South Bačka District, Vojvodina, Serbia. Red line represents January isotherm of +5 °C mean air temperature after Stanners & Bourdeau [84]. In cases of two or more too close localities, some are omitted with regard of a map scale.

It is surprising that a fungal species with such a large stromata could be left unrecorded in the second half of the 20th century in mycologically well-explored regions and countries (e.g., USA, Japan, Europe). Croatian mycologist Milica Tortić paid special attention to

lignicolous fungi without any *Entonaema* records during her long and diligent fieldwork, spanning the 1960s to the end of 20th century. The second author conducted a series of detailed fieldwork sessions during 1990s exactly in the same area and the habitat type (oak-ash flood forest, Crna Mlaka) where *E. cinnabarinum* was first recorded only later in 2009, also without noticing it. Therefore, on the basis of rather abundant recent records of *E. cinnabarinum* in Europe, and the ascertained global image of the species' ecological traits, we can assume that this species has been spreading from its most humid-thermophilic European strongholds into new western and southeastern European areas on the account of global warming effects [83].

Owing to a series of eight mild winters (2015/2016–2022/2023) in the above-mentioned European areas for *E. cinnabarinum*, and in the midwestern USA along main watercourses for *E. liquescens* (Britt Bunyard *pers. comm.*), this species could be able to overwinter. This was followed by successful stomatal development during unusually warm summer and autumnal months (Figure 6), after which the species was capable of conquering new available substrates in the forests of other areas via sporulation. The species' capability to actively spread, overwinter, and to withstand drying conditions and direct UV radiation could be significantly enhanced by its forcible discharge of ascospores via turgor of the living asci, as well as by the small volume of ascospores and the wall, equipped with melanins, that are also richly developed in the stomatal crust and perithecial walls (cf. [85]). This capability is also enhanced by the species' preference for coarse woody debris as a substrate (significant water containers) and the humid forest habitat types, as well as by a development of large stomata equipped with voluminous gelatinous interior capable of accumulating and preserving water transported from the substrate. This enables the fungus to use this water against drying and to keep full turgor in the ascogenous system during the warmest periods when the evaporation is highest, and at the same time, when the organism could only develop ascospores in temperate areas (Figure 6). This internal stomatal liquor, similar as in *Xylaria mesenterica*, could be homologous in origin and/or the function as the internal stomatal tissue of *Daldinia* spp. [86].

Finally, the authors herein wish to draw attention to the emergence of erroneous data in the GBIF (www.gbif.org, accessed on 26 June 2023) portal about the occurrence of *E. cinnabarinum* in eastern Croatia. The actual material (CNF 2/11267) discussed was collected from a completely different geographic area and was uploaded to iNaturalist (www.inaturalist.org, accessed on 26 June 2023 [87]) by someone else who was unfamiliar with the material's true origin. When compiling an overview on the distribution of a given fungal species, one should take great caution with regard to adopting electronic data since those not accompanied by sufficient evidence about the origin and species identity could include uncontrollable errors. Erroneous data about *Entonaema* species distribution were earlier discussed by Rogers [5].

5. Conclusions

Six species of *Entonaema* have been formally accepted to date, the type species *E. liquescens*, *E. cinnabarinum*, *E. dengii*, *E. moluccanum*, *E. globosum*, and *E. siamensis*. Prior to this study, the ITS sequence was available for only one true *Entonaema* (*E. liquescens* S.D. Russell iNaturalist # 91210856), but had not been published or phylogenetically analysed. In this study, four gene regions (ITS, LSU, *rpb2*, β -*tub*) of the four Croatian collections (CNF 2/11046, 2/11047, 2/11052, 2/11053) of *E. cinnabarinum* and one (American) collection of *E. liquescens* (CNF 2/11263) were sequenced for the first time. The results of this study reveal a true phylogenetic position of the genus *Entonaema* within the *Hypoxyloaceae*.

Judging from available data, dominant tree hosts in Europe for *E. cinnabarinum* are *Fraxinus* species (*F. angustifolia* in the Pannonian area and in Bulgarian longose, *F. excelsior* in the French Pyrénées Atlantiques), as well as *Quercus robur* in the Pannonian area. Being the (co-)dominant tree species in suitable flood and alluvial forests, those tree species may have served as the species' 'host bridge' for recent colonisation of the European humid warm temperate areas. In the midwestern USA, the most frequently mentioned hosts were

Quercus spp., which could have represented the ‘host bridge’ for *E. liquescens* in the species’ spreading from the most southeastern USA species’ strongholds towards the north via the Mississippi River and its tributaries. However, the analysed worldwide data prove that the two most frequent *Entonaema* species (*E. liquescens* and *E. cinnabarinum*) are plurivorous lignicolous saprotrophs. Therefore, we could expect the fungal adaptation to some other tree species growing under adequate climatic regime in suitable humid forest habitats in the future.

As for the rest of the *Entonaema* species, both *E. liquescens* and *E. cinnabarinum* were often considered subtropical–tropical species in the earliest papers (compare [68,73]). They are present in the areas under several types of warm temperate climate: Cfa—USA, Europe, Japan, Brazil; Cfb—Brazil, Ecuador; Csa—Spain; Cwa—Argentina, India, Mexico; Cwb—Mexico, Nepal. However, it is evident that both species were regularly recorded in the temperate zones of USA and Europe beginning only in the 21st century, on the well explored areas where those species have never been recorded before. Moreover, the apparent spread of these two *Entonaema* species during the last decade into the areas under (formerly) cooler temperate climate is in line with predicted climatic shift in Europe and North America [88] when we compare the current distribution of Köppen–Geiger climatic types in Europe, based on a period 1951–2000 [30], with the area that these climatic types would presumably cover during the period 2076–2100 [88]. Therefore, both *E. liquescens* and *E. cinnabarinum* could be good candidates for bioindicator species of climate change, especially because both are easily visible and recognizable by trained observers. Their appearance in the areas where they did not previously appear, could point to biologically effective climatic shifting along the border of a given cooler climatic type into a warmer, but the otherwise similar climatic type, e.g., Dfa or Cfb into Cfa (northwest Croatia and Hungary); Dfb (Nebraska, Iowa, northern Illinois and Indiana in the USA) or Dwb (Russian Far East) into a Cfa (Figure 6).

Author Contributions: Conceptualization, A.P., N.M. and I.K.; methodology, A.P., I.K. and N.M.; formal analysis, A.P., N.M. and I.K.; investigation, A.P., N.M., I.K., Z.T. and A.M.; resources, N.M., I.K., Z.T. and A.M.; data curation, A.P., N.M. and I.K.; writing—original draft preparation, A.P., N.M. and I.K.; writing—review and editing, A.P., N.M., I.K., Z.T. and A.M.; visualization, A.P., N.M. and I.K.; supervision, I.K., N.M., A.M. and Z.T.; project administration, A.M.; funding acquisition, A.M., I.K., N.M. All authors have read and agreed to the published version of the manuscript.

Funding: This work was fully supported by the Croatian Science Foundation under the project grants ForFungiDNA HRZZ-IP-2018-01-1736 (to A.P., I.K., N.M., A.M., Z.T.), and HRZZ-DOK-2018-09-7081 (to A.P.).

Data Availability Statement: All sequences used in this study are available in GenBank. Alignments and phylogenetic trees generated in this study are available at Zenodo (DOI: 10.5281/zenodo.8302699).

Acknowledgments: We thank Milan Čerkez, Juraj Marković and Matija Josipović for their fieldwork effort and providing the collections of *Entonaema cinnabarinum*. Trent Gonzales and Britt Bunyard are appreciated for sampling and delivery of *E. liquescens* from the USA. The authors are grateful to Britt Bunyard for making improvements to the English text.

Conflicts of Interest: The authors declare no conflict of interest. The funder had no role in the design of the study; in the collection, analyses, or interpretation of data; in the writing of the manuscript, or in the decision to publish the results.

References

1. Möller, A. *Phycomyceten Und Ascomyceten. Untersuchungen Aus Brasilien*; Bot. Mitth. Tropen, Heft 9; G. Fischer: Jena, Germany, 1901.
2. Stadler, M.; Fournier, J.; Læssøe, T.; Lechat, C.; Tichy, H.-V.; Piepenbring, M. Recognition of hypoxylid and xylarioid *Entonaema* species and allied *Xylaria* species from a comparison of holomorphic morphology, HPLC profiles, and ribosomal DNA sequences. *Mycol. Prog.* **2008**, *7*, 53–73. [CrossRef]
3. Lloyd, C.G. *Mycological Notes*, No. 69. *Mycol. Writ.* **1923**, *7*, 1185–1218.

4. Martin, G.W. New or Noteworthy Fungi from Panama and Columbia. II. *Mycologia* **1938**, *30*, 431–441. [[CrossRef](#)]
5. Rogers, J.D. *Sarcoxyton* and *Entonaema* (Xylariaceae). *Mycologia* **1981**, *73*, 26–61. [[CrossRef](#)]
6. Rogers, J.D. *Entonaema liquescens*: Description of the Anamorph and Thoughts on Its Systematic Position. *Mycotaxon* **1982**, *15*, 500–506.
7. Eriksson, O.E.; Hawksworth, D.L. Outline of the Ascomycetes—1993. *Syst. Ascomycetum* **1993**, *12*, 51–257.
8. Whalley, A. The xylariaceous way of life. *Mycol. Res.* **1996**, *100*, 897–922. [[CrossRef](#)]
9. Ju, Y.-M.; Rogers, J.D. *A Revision of the Genus Hypoxylon*; APS Press: St Paul, MN, USA, 1996.
10. Wendt, L.; Sir, E.B.; Kuhnert, E.; Heitkämper, S.; Lambert, C.; Hladki, A.I.; Romero, A.I.; Luangsa-ard, J.J.; Srikritikulchai, P.; Peršoh, D.; et al. Resurrection and emendation of the Hypoxylaceae, recognised from a multigene phylogeny of the Xylariales. *Mycol. Prog.* **2018**, *17*, 115–154. [[CrossRef](#)]
11. Cooke, M.C. Some Australian Fungi. *Grevillea* **1887**, *15*, 93–101.
12. Heim, R. Quelques Ascomycètes Remarquables, II.—Le Genre *Entonaema* Möll. Au Mexique. *Bull. Trimest. Société Mycol. De Fr.* **1960**, *76*, 121–129.
13. Sihanonth, P.; Thienhirun, S.; Whalley, A.J. *Entonaema* in Thailand. *Mycol. Res.* **1998**, *102*, 458–460. [[CrossRef](#)]
14. Triebel, D.; Peršoh, D.; Wollweber, H.; Stadler, M. Phylogenetic relationships among *Daldinia*, *Entonaema*, and *Hypoxylon* as inferred from ITS nrDNA analyses of Xylariales. *Nova Hedwig.* **2005**, *80*, 25–43. [[CrossRef](#)]
15. Wibberg, D.; Stadler, M.; Lambert, C.; Bunk, B.; Spröer, C.; Rückert, C.; Kalinowski, J.; Cox, R.J.; Kuhnert, E. High quality genome sequences of thirteen Hypoxylaceae (Ascomycota) strengthen the phylogenetic family backbone and enable the discovery of new taxa. *Fungal Divers.* **2020**, *106*, 7–28. [[CrossRef](#)]
16. Baral, H.O. Vital versus Herbarium Taxonomy: Morphological Differences between Living and Dead Cells of Ascomycetes, and Their Taxonomic Implications. *Mycologia* **1992**, *44*, 333–390.
17. Henriot, A.; Cheype, J.-L. Piximètre: La Mesure de Dimensions Sur Images. Version 5.10 R1541. Available online: <http://ach.log.free.fr/Piximetre> (accessed on 1 October 2020).
18. Samson, R.A.; Hoekstra, E.S.; Frisvad, J.C.; Filtenborg, O. *Introduction to Foodborne Fungi*; Centraalbureau voor Schimmelcultures: Baarn, The Netherlands; Delft, The Netherlands, 1996.
19. Gardes, M.; Bruns, T.D. ITS primers with enhanced specificity for basidiomycetes—Application to the identification of mycorrhizae and rusts. *Mol. Ecol.* **1993**, *2*, 113–118. [[CrossRef](#)] [[PubMed](#)]
20. White, T.J.; Bruns, T.; Lee, S.; Taylor, J. Amplification and direct sequencing of fungal ribosomal RNA genes for phylogenetics. In *PCR Protocols: A Guide to Methods and Applications*; Innis, M.A., Gelfand, D.H., Sninsky, J.J., White, T.J., Eds.; Academic Press: San Diego, CA, USA, 1990; pp. 315–322.
21. Vilgalys, R.; Hester, M. Rapid genetic identification and mapping of enzymatically amplified ribosomal DNA from several *Cryptococcus* species. *J. Bacteriol.* **1990**, *172*, 4238–4246. [[CrossRef](#)]
22. Liu, Y.J.; Whelen, S.; Hall, B.D. Phylogenetic relationships among ascomycetes: Evidence from an RNA polymerase II subunit. *Mol. Biol. Evol.* **1999**, *16*, 1799–1808. [[CrossRef](#)]
23. O'Donnell, K.; Cigelnik, E. Two Divergent Intragenomic rDNA ITS2 Types within a Monophyletic Lineage of the Fungus *Fusarium* are Nonorthologous. *Mol. Phylogenetics Evol.* **1997**, *7*, 103–116. [[CrossRef](#)]
24. Kazutaka, K.; Misakwa, K.; Kei-ichi, K.; Miyata, T. MAFFT: A novel method for rapid multiple sequence alignment based on fast Fourier transform. *Nucleic Acids Res.* **2002**, *30*, 3059–3066. [[CrossRef](#)]
25. Katoh, K.; Standley, D.M. MAFFT Multiple Sequence Alignment Software Version 7: Improvements in Performance and Usability. *Mol. Biol. Evol.* **2013**, *30*, 772–780. [[CrossRef](#)]
26. Nguyen, L.-T.; Schmidt, H.A.; Von Haeseler, A.; Minh, B.Q. IQ-TREE: A Fast and Effective Stochastic Algorithm for Estimating Maximum-Likelihood Phylogenies. *Mol. Biol. Evol.* **2015**, *32*, 268–274. [[CrossRef](#)] [[PubMed](#)]
27. Trifinopoulos, J.; Nguyen, L.-T.; von Haeseler, A.; Minh, B.Q. W-IQ-TREE: A fast online phylogenetic tool for maximum likelihood analysis. *Nucleic Acids Res.* **2016**, *44*, W232–W235. [[CrossRef](#)]
28. Huelsenbeck, J.P.; Ronquist, F. MRBAYES: Bayesian inference of phylogenetic trees. *Bioinformatics* **2001**, *17*, 754–755. [[CrossRef](#)]
29. Letunic, I.; Bork, P. Interactive Tree Of Life (iTOL) v5: An online tool for phylogenetic tree display and annotation. *Nucleic Acids Res.* **2021**, *49*, W293–W296. [[CrossRef](#)] [[PubMed](#)]
30. Kottke, M.; Grieser, J.; Beck, C.; Rudolf, B.; Rubel, F. World map of the Köppen-Geiger climate classification updated. *Meteorol. Z.* **2006**, *15*, 259–263. [[CrossRef](#)] [[PubMed](#)]
31. Hsieh, H.-M.; Lin, C.-R.; Fang, M.-J.; Rogers, J.D.; Fournier, J.; Lechat, C.; Ju, Y.-M. Phylogenetic status of *Xylaria* subgenus *Pseudoxylaria* among taxa of the subfamily Xylarioideae (Xylariaceae) and phylogeny of the taxa involved in the subfamily. *Mol. Phylogenetics Evol.* **2010**, *54*, 957–969. [[CrossRef](#)]
32. Kuhnert, E.; Sir, E.B.; Lambert, C.; Hyde, K.D.; Hladki, A.I.; Romero, A.I.; Rohde, M.; Stadler, M. Phylogenetic and chemotaxonomic resolution of the genus *Annulohypoxylon* (Xylariaceae) including four new species. *Fungal Divers.* **2016**, *85*, 1–43. [[CrossRef](#)]
33. Kuhnert, E.; Fournier, J.; Peršoh, D.; Luangsa-Ard, J.J.D.; Stadler, M. New *Hypoxylon* species from Martinique and new evidence on the molecular phylogeny of *Hypoxylon* based on ITS rDNA and β -tubulin data. *Fungal Divers.* **2013**, *64*, 181–203. [[CrossRef](#)]
34. Daranagama, D.A.; Camporesi, E.; Tian, Q.; Liu, X.; Chamyuang, S.; Stadler, M.; Hyde, K.D. *Anthostomella* is polyphyletic comprising several genera in Xylariaceae. *Fungal Divers.* **2015**, *73*, 203–238. [[CrossRef](#)]

35. Li, Q.R.; Kang, J.C.; Hyde, K.D. Two new species of the genus *Collodiscula* (Xylariaceae) from China. *Mycol. Prog.* **2015**, *14*, 52. [CrossRef]
36. Bitzer, J.; Læssøe, T.; Fournier, J.; Kummer, V.; Decock, C.; Tichy, H.-V.; Piepenbring, M.; Peršoh, D.; Stadler, M. Affinities of Phylacia and the daldinoid Xylariaceae, inferred from chemotypes of cultures and ribosomal DNA sequences. *Mycol. Res.* **2008**, *112*, 251–270. [CrossRef]
37. Hsieh, H.-M.; Ju, Y.-M.; Rogers, J.D. Molecular phylogeny of *Hypoxylon* and closely related genera. *Mycologia* **2005**, *97*, 844–865. [CrossRef] [PubMed]
38. Stadler, M.; Læssøe, T.; Fournier, J.; Decock, C.; Schmieschek, B.; Tichy, H.-V.; Peršoh, D. A polyphasic taxonomy of *Daldinia* (Xylariaceae). *Stud. Mycol.* **2014**, *77*, 1–143. [CrossRef] [PubMed]
39. Johannesson, H.; Læssøe, T.; Stenlid, J. Molecular and morphological investigation of *Daldinia* in northern Europe. *Mycol. Res.* **2000**, *104*, 275–280. [CrossRef]
40. Spatafora, J.W.; Sung, G.-H.; Johnson, D.; Hesse, C.; O’rourke, B.; Serdani, M.; Spotts, R.; Lutzoni, F.; Hofstetter, V.; Miadlikowska, J.; et al. A five-gene phylogeny of Pezizomycotina. *Mycologia* **2006**, *98*, 1018–1028. [CrossRef]
41. *Entonaema Liquescens*. iNaturalist. Available online: <https://www.inaturalist.org/taxa/350744-Entonaema-liquescens> (accessed on 25 April 2023).
42. Gazis, R.; Chaverri, P. Diversity of fungal endophytes in leaves and stems of wild rubber trees (*Hevea brasiliensis*) in Peru. *Fungal Ecol.* **2010**, *3*, 240–254. [CrossRef]
43. Skaltsas, D.N.; Badotti, F.; Vaz, A.B.M.; da Silva, F.F.; Gazis, R.; Wurdack, K.; Castlebury, L.; Góes-Neto, A.; Chaverri, P. Exploration of stem endophytic communities revealed developmental stage as one of the drivers of fungal endophytic community assemblages in two Amazonian hardwood genera. *Sci. Rep.* **2019**, *9*, 12685. [CrossRef]
44. Higginbotham, S.; Wong, W.R.; Lington, R.G.; Spatafora, C.; Iturrado, L.; Arnold, A.E. Sloth Hair as a Novel Source of Fungi with Potent Anti-Parasitic, Anti-Cancer and Anti-Bacterial Bioactivity. *PLoS ONE* **2014**, *9*, e84549. [CrossRef]
45. Kim, C.S.; Jo, J.W.; Kwag, Y.-N.; Sung, G.-H.; Lee, S.-G.; Kim, S.-Y.; Shin, C.-H.; Han, S.-K. Mushroom Flora of Ulleung-gun and a Newly Recorded Bovista Species in the Republic of Korea. *Mycobiology* **2015**, *43*, 239–257. [CrossRef]
46. Zhang, N.; Castlebury, L.A.; Miller, A.N.; Huhndorf, S.M.; Schoch, C.L.; Seifert, K.A.; Rossman, A.Y.; Rogers, J.D.; Kohlmeyer, J.; Volkmann-Kohlmeyer, B.; et al. An overview of the systematics of the Sordariomycetes based on a four-gene phylogeny. *Mycologia* **2006**, *98*, 1076–1087. [CrossRef]
47. Koukol, O.; Kelnarová, I.; Černý, K. Recent observations of sooty bark disease of sycamore maple in Prague (Czech Republic) and the phylogenetic placement of *Cryptostroma corticale*. *For. Pathol.* **2014**, *45*, 21–27. [CrossRef]
48. Pourmoghammad, M.J.; Lambert, C.; Surup, F.; Khodaparast, S.A.; Krisai-Greilhuber, I.; Voglmayr, H.; Stadler, M. Discovery of a new species of the *Hypoxylon rubiginosum* complex from Iran and antagonistic activities of *Hypoxylon* spp. against the Ash Dieback pathogen, *Hymenoscyphus fraxineus*, in dual culture. *Mycoskeys* **2020**, *66*, 105–133. [CrossRef]
49. Ma, H.-X.; Qiu, J.-Z.; Xu, B.; Li, Y. Two *Hypoxylon* species from Yunnan Province based on morphological and molecular characters. *Phytotaxa* **2018**, *376*, 27–36. [CrossRef]
50. Cedeño-Sánchez, M. Three new species of *Hypoxylon* and new records of Xylariales from Panama. *Mycosphere* **2020**, *11*, 1457–1476. [CrossRef]
51. Ma, H.; Song, Z.; Pan, X.; Li, Y.; Yang, Z.; Qu, Z. Multi-Gene Phylogeny and Taxonomy of *Hypoxylon* (Hypoxylaceae, Ascomycota) from China. *Diversity* **2022**, *14*, 37. [CrossRef]
52. Song, Z.-K.; Zhu, A.-H.; Liu, Z.-D.; Qu, Z.; Li, Y.; Ma, H.-X. Three New Species of *Hypoxylon* (Xylariales, Ascomycota) on a Multigene Phylogeny from Medog in Southwest China. *J. Fungi* **2022**, *8*, 500. [CrossRef]
53. Lambert, C.; Pourmoghammad, M.J.; Cedeño-Sánchez, M.; Surup, F.; Khodaparast, S.A.; Krisai-Greilhuber, I.; Voglmayr, H.; Stradal, T.E.B.; Stadler, M. Resolution of the *Hypoxylon fuscum* Complex (Hypoxylaceae, Xylariales) and Discovery and Biological Characterization of Two of Its Prominent Secondary Metabolites. *J. Fungi* **2021**, *7*, 131. [CrossRef]
54. Stadler, M.; Kuhnert, E.; Peršoh, D.; Fournier, J. The Xylariaceae as Model Example for a Unified Nomenclature Following the “One Fungus-One Name” (1F1N) Concept. *Mycology* **2013**, *4*, 5–21. [CrossRef]
55. Dai, D.Q.; Phookamsak, R.; Wijayawardene, N.N.; Li, W.J.; Bhat, D.J.; Xu, J.C.; Taylor, J.E.; Hyde, K.D.; Chukeatirote, E. Bambusicolous fungi. *Fungal Divers.* **2016**, *82*, 1–105. [CrossRef]
56. Bills, G.F.; González-Menéndez, V.; Martín, J.; Platas, G.; Fournier, J.; Peršoh, D.; Stadler, M. *Hypoxylon pulicicidum* sp. nov. (Ascomycota, Xylariales), a Pantropical Insecticide-Producing Endophyte. *PLoS ONE* **2012**, *7*, e46687. [CrossRef]
57. Sir, E.B.; Becker, K.; Lambert, C.; Bills, G.F.; Kuhnert, E. Observations on Texas hypoxylons, including two new *Hypoxylon* species and widespread environmental isolates of the *H. croceum* complex identified by a polyphasic approach. *Mycologia* **2019**, *111*, 832–856. [CrossRef] [PubMed]
58. Pi, Y.-H.; Zhang, X.; Liu, L.-L.; Long, Q.-D.; Shen, X.-C.; Kang, Y.-Q.; Hyde, K.D.; Boonmee, S.; Kang, J.-C.; Li, Q.-R. Contributions to species of Xylariales in China—4. *Hypoxylon wujiangensis* sp. nov. *Phytotaxa* **2020**, *455*, 21–30. [CrossRef]
59. Samarakoon, M.C.; Hyde, K.D.; Maharachchikumbura, S.S.N.; Stadler, M.; Jones, E.B.G.; Promputtha, I.; Suwannarach, N.; Camporesi, E.; Bulgakov, T.S.; Liu, J.-K. Taxonomy, phylogeny, molecular dating and ancestral state reconstruction of Xylariomycetidae (Sordariomycetes). *Fungal Divers.* **2022**, *112*, 1–88. [CrossRef]
60. Pažoutová, S.; Šrůtka, P.; Holuša, J.; Chudičková, M.; Kolařík, M. The phylogenetic position of *Obolarina dryophila* (Xylariales). *Mycol. Prog.* **2010**, *9*, 501–507. [CrossRef]

61. Senanayake, I.C.; Maharachchikumbura, S.S.N.; Hyde, K.D.; Bhat, J.D.; Jones, E.B.G.; McKenzie, E.H.C.; Dai, D.Q.; Daranagama, D.A.; Dayarathne, M.C.; Goonasekara, I.D.; et al. Towards unraveling relationships in Xylariomycetidae (Sordariomycetes). *Fungal Divers.* **2015**, *73*, 73–144. [[CrossRef](#)]
62. Peláez, F.; González, V.; Platas, G.; Sánchez-Ballesteros, J.; Rubio, V. Molecular Phylogenetic Studies within the Xylariaceae Based on Ribosomal DNA Sequences. *Fungal Divers.* **2008**, *31*, 111–134.
63. Tang, A.M.C.; Jeewon, R.; Hyde, K.D. A Re-Evaluation of the Evolutionary Relationships within the Xylariaceae Based on Ribosomal and Protein-Coding Gene Sequences. *Fungal Divers.* **2009**, *34*, 127–155.
64. Stadler, M.; Flessa, F.; Rambold, G.; Peršoh, D.; Fournier, J.; Læssøe, T.; Chlebicki, A.; Lechat, C. Chemotaxonomic and phylogenetic studies of *Thamnomycetes* (Xylariaceae). *Mycoscience* **2010**, *51*, 189–207. [[CrossRef](#)]
65. Ju, Y.-M.; Hsieh, H.-M. Xylaria species associated with nests of *Odontotermes formosanus* in Taiwan. *Mycologia* **2007**, *99*, 936–957. [[CrossRef](#)]
66. Ju, Y.-M.; Hsieh, H.-M.; Rogers, J.D.; Fournier, J.; Jaklitsch, W.M.; Courtecuisse, R. New and interesting penzigoid *Xylaria* species with small, soft stromata. *Mycologia* **2012**, *104*, 766–776. [[CrossRef](#)] [[PubMed](#)]
67. Sir, E.; Stadler, M. A new species of *Daldinia* (Xylariaceae) from the Argentine subtropical montane forest. *Mycosphere* **2016**, *7*, 1378–1388. [[CrossRef](#)]
68. Fintha, G.; Benedek, L.; Orbán, S. New Macrofungial Record in Hungary: *Entonaema cinnabarinum* (Cooke & Masee) Lloyd. *Acta Biol. Plant. Agriensis* **2019**, *7*, 127–130. [[CrossRef](#)]
69. Rogers, J.D.; San Martín, F.; Ju, Y.-M. Mexican Fungi: *Xylaria entosulphurea* Sp. Nov. and Neotypification of *Entonaema globosum*. *Mycotaxon* **1996**, *58*, 483–487.
70. Stadler, M.; Ju, Y.-M.; Rogers, J.D. Chemotaxonomy of *Entonaema*, *Rhopalostroma* and other Xylariaceae. *Mycol. Res.* **2004**, *108*, 239–256. [[CrossRef](#)]
71. Patouillard, N. Champignons de La Nouvelle-Calédonie. *Bull. Trimest. Société Mycol. De Fr.* **1911**, *27*, 329–333.
72. Benkert, D. *Kotlabaea macrospora* Benkert nov. sp. und einige weitere bemerkenswerte Ascomyceten aus Bulgarien Mit einer Abbildung. *Feddes Repert.* **1993**, *104*, 547–549. [[CrossRef](#)]
73. Fedosova, A.G. The New Record of *Entonaema cinnabarinum* (Xylariaceae, Ascomycota) in Europe. *Vestnik of Saint Petersburg University. Series 3. Biology* **2012**, *1*, 10–13.
74. Harkevich, S.S. (Ed.) флора и Растительность Уссурийского Заповедника; Наука: Moscow, Russia, 1978.
75. Azbukina, Z.M.; Bardunov, L.V.; Bezdeleva, T.A.; Bogacheva, A.V.; Bulakh, E.M.; Vasilyeva, L.N.; Govorova, O.K.; Egorova, L.N.; Zhabyko, E.V.; Nikulina, T.V.; et al. *Flora, Vegetation and Mycobiota of the Reserve "Ussuriysky"*; Daljnauka: Vladivostok, Russia, 2006.
76. Sánchez-Jácume, M.; Guzmán-Dávalos, L. New Records of Ascomycetes from Jalisco, Mexico. *Mycotaxon* **2005**, *92*, 177–191.
77. Quang, D.N.; Stadler, M.; Fournier, J.; Asakawa, Y. Carneic Acids A and B, Chemotaxonomically Significant Antimicrobial Agents from the Xylariaceous Ascomycete *Hypoxylon carneum*. *J. Nat. Prod.* **2006**, *69*, 1198–1202. [[CrossRef](#)]
78. Helaly, S.E.; Thongbai, B.; Stadler, M. Diversity of biologically active secondary metabolites from endophytic and saprotrophic fungi of the ascomycete order Xylariales. *Nat. Prod. Rep.* **2018**, *35*, 992–1014. [[CrossRef](#)]
79. Lücking, R.; Aime, M.C.; Robbertse, B.; Miller, A.N.; Aoki, T.; Ariyawansa, H.A.; Cardinali, G.; Crous, P.W.; Druzhinina, I.S.; Geiser, D.M.; et al. Fungal taxonomy and sequence-based nomenclature. *Nat. Microbiol.* **2021**, *6*, 540–548. [[CrossRef](#)]
80. Zamora, J.C.; Svensson, M.; Kirschner, R.; Olariaga, I.; Ryman, S.; Parra, L.A.; Geml, J.; Rosling, A.; Adamčík, S.; Ahti, T.; et al. Considerations and consequences of allowing DNA sequence data as types of fungal taxa. *IMA Fungus* **2018**, *9*, 167–175. [[CrossRef](#)]
81. Šrůtka, P.; Pažoutová, S.; Kolařík, M. *Daldinia decipiens* and *Entonaema cinnabarina* as fungal symbionts of Xiphydria wood wasps. *Mycol. Res.* **2007**, *111*, 224–231. [[CrossRef](#)]
82. Læssøe, T. *Entonaema cinnabarina*-En Eksotisk Kernesvamp. *Svampe* **1997**, *36*, 21–22.
83. Fintha, G.; Nagy, I.; Vitkó, T.; Benedek, L.; Baranyai, G. Az Ócsai Turjánvidék Natura 2000-es kijelölt területeinek nagygyombái. *J. Landscape Ecol.* **2022**, *20*, 3–21. [[CrossRef](#)]
84. Stanners, D.; Bourdeau, P. *Europe's Environment: The Dobříš Assessment*; European Environment Agency: Copenhagen, Denmark, 1995.
85. Quijada, L.; Matočec, N.; Kušan, I.; Tanney, J.B.; Johnston, P.R.; Mešić, A.; Pfister, D.H. Apothecial Ancestry, Evolution, and Re-Evolution in *Thelebolales* (Leotiomyces, Fungi). *Biology* **2022**, *11*, 583. [[CrossRef](#)] [[PubMed](#)]
86. Ju, Y.M.; Rogers, J.D.; San Martín, F. A Revision of the Genus *Daldinia*. *Mycotaxon* **1997**, *61*, 243–293.
87. INaturalist Research-Grade Observations. Available online: <https://www.inaturalist.org> (accessed on 26 June 2023).
88. Rubel, F.; Kotteck, M. Observed and projected climate shifts 1901–2100 depicted by world maps of the Köppen-Geiger climate classification. *Meteorol. Z.* **2010**, *19*, 135–141. [[CrossRef](#)]

Disclaimer/Publisher's Note: The statements, opinions and data contained in all publications are solely those of the individual author(s) and contributor(s) and not of MDPI and/or the editor(s). MDPI and/or the editor(s) disclaim responsibility for any injury to people or property resulting from any ideas, methods, instructions or products referred to in the content.